SINGLE-CHANNEL PROPERTIES OF EPISODIC ATAXIA TYPE 1 (EA-1) MUTATIONS IN THE HUMAN VOLTAGE-GATED POTASSIUM CHANNELS (hKv1.1)

by

Zhaoping Liu

Presented to the Department of Physiology and Pharmacology
and Oregon Health Sciences University
School of Medicine
in partial fulfillment of
the requirements for the degree of
Master of Science
June 2001

School of Medicine

Oregon Health Sciences University

CERFIFICATE OF APPROVAL

This is to certify that the thesis of

Zhaoping Liu

has been approved

[redacted]

Professor in charge of thesis

[redacted]

Member

[redacted]

Member

[redacted]

Member

[redacted]

Member

TABLE OF CONTENTS

LIST OF FIGURES

ACKNOWLEDGMENTS

I am very fortunate to have two great talented scientists: Drs. James Maylie and John Adelman. With their great encouragement and support, I am able to go so far. Their extraordinary insights into science and compensatory talents greatly helped my research. Dr. James Maylie taught me excellent techniques in electrophysiology and computer as well as personal properties such as honesty and integrity. Dr. John Adelman gave me lessons on how to be an excellent molecular biologist as well as on how to devote all my efforts to work (to be a real workaholic!).

I owe much to Drs. Sarah Appel and Mark Brodie for their understanding and support financially and academically. Thanks to Dr. John Solaro for his leadership and wonderful financial support.

I am indebted to Christ Bond, Xiaoming Xia, Patricia Zerr, Kevin Gibson, Taka Ishii and all the people who helped me during my study.

Department of Physiology and Pharmacology provides me with great study environment and opportunity. I feel grateful to be a member of it.

I am also grateful that I have a great family. My wife is always my great supporter rain or shine. My parents have been to the U.S.A. several times to help us take care of our kids.

ABSTRACT

Subunits of the voltage-gated potassium channel Kv1.1 containing mutations responsible for episodic ataxia type 1 (EA-1), an autosomal dominant neurological disorder, were expressed in *Xenopus* oocyte and their single-channel properties were studied. Single-channel recordings from the expressed channels were made using the cell-free inside-out patch-clamp method. Single-channel current analysis showed that two EA-1 mutations E325D and V408A, residing on opposite sides of the deep pore in S5 and S6, respectively, decreased the channel open probability significantly, from 0.75 for wild type to 0.53 for V408A, to 0.52 for E325D, but had no effect on single-channel conductance compared with wild type. The single-channel conductance (pS) for wild type, E325D and V408A was 10.48 ± 0.459 (n=5), 10.467 ± 0.786 (n=3) and 10.00 ± 0.577 (n=3), respectively ($P>0.05$). The first latency time constants at different voltages were compared between wild type and EA-1 mutations. V408A channels had fastest activation, wild type channels had slowest activation, E325D channels in between. These results were consistent with the two-electrode voltage-clamp study (Adelman, Bond, Pessia and Maylie, 1995; Zerr, Adelman and Maylie, 1998) in which EA-1 mutations, V408A and E325D, had much faster activation than wild type channels. Transitions after first opening are voltage-independent at depolarized

voltages. Wild type and EA-1 mutations all have 3 components. There is no difference between wild type and V408A or E325D channels. The fast component, 0.3 ms in duration, can be seen as flicker closings in the single channel records. These closings represent the most frequently observed closed events, over 70% of the closures. The intermediate component of the distribution of closed durations is 1 to 5 ms in duration and comprises about 30% of the closures. In contrast to the fast and intermediate components, the slow component is frequently not significant at depolarized voltages and is more prevalent in the activation voltage range, at ¨ 40 mV and ¨ 60 mV, than at the depolarized voltages. In all patches the open events elicited by steps to voltages between ¨ 60 and +50 mV were sufficiently described by a single exponential distribution and did not warrant a distribution containing two components. This suggests that only a single open conformation is kinetically distinguishable in the wild type, E325D and V408A. More importantly, these two EA-1 mutations decreased open time constants dramatically and caused the latter became voltage-dependent. Taken together, these results showed that EA-1 mutations, E325D and V408A, decreased the open probability and destabilized open state.

INTRODUCTION

Episodic Ataxia

Episodic ataxia (EA), which was first described by Gancher and Nutt (1986) at Oregon Health Science University, is a rare autosomal dominant neurological disorder that affects both peripheral and central nervous systems. Affected individuals experience attacks of generalized ataxia brought on by physical or emotional stress, with only minimal neurological abnormalities between attacks (Gancher and Nutt, 1986; Brunt and van Weerden, 1990). Families with autosomal dominant EA appear to represent two clinically distinct types.

Episodic ataxia type 1 (EA-1) is characterized by brief episodes of imbalance and cognitive symptoms typically lasting seconds to minutes. During and between attacks, patients experience spontaneous, repetitive twitchings in distal musculature, usually around the eyes or in the hands (myokymia) that arise from peripheral nerves. Onset occurs in early childhood and exhibits a high degree of penetrance (Browne, Gancher, Nutt, Brunt, Smith, Kramer and Litt, 1994). Clinically, EA-1 can be differentiated from EA-2 by the shorter duration of attacks, the presence of myokymia (twitching of the small muscles around the eyes or in the hands), and the absence of interictal ataxia, nystagmus and cerebellar vermis atrophy (Griggs and Nutt, 1995). Table 1 shows the

difference between the two forms of episodic ataxia.

Table 1. Autosomal Dominant Episodic Ataxia

	EA-1*	EA-2*
Chromosome location	12p13	19p13.1
Gene lesion	K^+ channel gene (KCNA1 mutations	Ca^{2+} channel gene (CACNL1A4) mutations
Duration of attacks	Seconds to minutes	Hours to days
Provoking factors	Startle, exercise	Stress, exercise, fatigue
Onset of attacks	Early childhood	Adolescence; late childhood
Associated findings	Myokymia; Joint contractures; Paroxysmal kinesiogenic choreoathetosis	Nystagmus; Headache; Developmental delay; Cerebellar vermian atrophy
Progressive cerebellar sign	No	Frequent
Treatment	Acetazolamide; phenytoin	Acetazolamide
Source	Litt, et al. (1994). Am J Hum Genet 55:702-709	Vahedi, et al. (1995). Ann Neurol 37: 289-293

** EA-1 = episodic ataxia type 1; EA-2 = episodic ataxia type 2*

Ion Channel Gene Mutations and Human Neurological Disorders

Molecular studies of ion channels have revealed a remarkable diversity of channel genes. Since the first Na^+ channel mutation disease, known as hyperkalemic periodic paralysis, was identified in 1990 (Fontaine, Khurana, Hoffman, Bruns, Haines, Trofatter, Hanson, Rich, McFarlane and Yasek), the genetic defects responsible for many inherited neuromuscular and ataxic syndromes have been identified and in many cases occur in the coding sequence of an ion channel gene (Cooper and Jan, 1999; Ashcroft, 2000; Celesia, 2001).

These disorders share two fascinating similarities: they are all episodic, frequently in people that are clinically totally normal between attacks. In addition they occur as the result of missense mutations in evolutionarily related genes.

Episodic Ataxia Is a Neurological Channelopathy

Channels have a fundamental role in neuronal signaling thus channel dysfunction may result in a variety of neurological disorders. Disorders of channel function are called channelopathies.

The first voltage-gated K^+ channel mutations known to cause a human disease were identified by Litt group in Oregon Health Sciences University in 1994 (Browne, Gancher, Nutt, Brunt, Smith, Kramer and Litt). Periodic ataxia caused by K^+ channel mutations now joins the family of other periodic neurologic disorders in humans that are known to result from mutations in Na^+ channels (Fontaine, Khurana, Hoffman, Bruns, Haines, Trofatter, Hanson, Rich, McFarlane and Yasek, 1990); Ca^{2+} channels (Ptacek, Tawil, Griggs, Engel, Layzer, Kwiecinski, McMains, Santiago, Moore and Fouad, 1994) and Cl^- channels (Koch, Steinmeyer, Lorenz, Ricker, Wolf, Otto, Zoll, Lehmann-Horn, Grezeschik and Jentsch, 1992). Patients with mutations in these three ion channels frequently have dramatic improvement of symptoms and prevention of attacks with carbonic

anhydrase inhibitors. The reason for this is not clear but likely relates to an effect common to voltage-gated cation channels---perhaps through alterations of the pH at the cell membrane.

Genetic linkage studies and molecular studies have localized the EA-1 syndrome locus to chromosome 12p13 (Litt, Kramer, Browne, Gancher, Brunt, Root, Phromchotikul, Dubay and Nutt, 1994) and, subsequently KCNA1, the gene encoding the voltage-gated delayed rectifier K^+ channel Kv1.1, was identified as underlying EA-1 (Browne, Gancher, Nutt, Brunt, Smith, Kramer and Litt, 1994; Browne, Brunt, Griggs, Nutt, Gancher, Smith and Litt, 1995). The mutations occur in positions highly conserved among the voltage-gated K^+ channel superfamily. In each affected family, a distinct missense point mutation has been identified in the coding sequence of Kv1.1, and all affected individuals are heterozygous.

The finding that Kv1.1 missense mutations underlie familial EA-1 presents analogies to the *Shaker* disorder in *Drosophila* (Kaplan and Trout, 1969). Physiological studies of *Drosophila* muscle cells revealed abnormalities in a rapidly inactivating K^+ current that led to the hypothesis that the *Shaker* locus is a K^+ channel gene. The *Shaker* locus from *Drosophila* was the first K^+ channel cloned and characterized at the molecular level (Kamb, Iverson, and Tanouye, 1987; Papazian, Schwarz, Tempel, Jan, and Jan, 1987). Kv1.1 was the first mammalian homologue cloned,

and expression of Kv1.1 in *Xenopus* oocytes results in a K^+ currents with delayed rectifier properties that lack the fast inactivation of the A-type current (Christie, Adelman, Douglass, and North, 1989; Stuhmer, Stocker, Sakman, Seeburg, Baumann, Grupe, Ackermann and Pongs, 1988).

The positions of the amino acids in Kv1.1 that have been linked to EA-1 are shown schematically in Figure 1 (Adelman, Bond, Pessia, and Maylie, 1995). The different locations of the various EA-1 point missense mutations suggest that they may affect distinct aspects of voltage-gated K^+ channels. Furthermore, they occur at positions that are highly conserved among the voltage-gated K^+ channel superfamily. Two mutations (V174F and F184C) reside in the first transmembrane domain, two (R239S and F249I) in the intracellular loop between the second and third transmembrane domain, one (E325D) at the cytoplasmic interface of fifth transmembrane domain, and one (V408A) in the C-terminal portion of sixth transmembrane domain.

Voltage-Dependent K^+ Channels

I. Ionic channels are pores

All cells maintain concentration gradients for inorganic ions between their interior and exterior. K^+ ion is at higher concentration in cytoplasm than extracellular fluid; Na^+ and Ca^{2+} ions exhibit the opposite distribution. In a typical mammalian cell, the intracellular K^+ concentration is 140 mM, Na^+ 12 mM and Ca^{2+} 10^{-7} M. Extracellularly, K^+ is typically 5 mM, Na^+ 140 mM and Ca^{2+} 2.4 mM (Hille, 1992; Ashcroft, 2000; Kandel, Schartz and Jessel, 2000).

These gradients make possible a system for electrical signaling based on the activity of ion channel proteins embedded in the cell membrane. Ion channels form pores that allow ions to move rapidly through cell membranes down their electrochemical gradients. It is evident that there will be some potential at which the electrical force on the ion exactly balances the opposing force of the concentration gradient. This potential is known as the equilibrium potential of the ion and it is given by the Nernst equation. For ion X,

$$E_x = (RT/zF) \ln([X]_o/[X]_i)$$

Where E_x is the equilibrium potential, R is the gas constant, T is the absolute temperature, z is the valency of the ion, and F is the Faraday constant. $[X]_o$ and $[X]_i$ are the external and internal concentration of the ion X, respectively.

With physiological K^+ concentrations given above, the calculated K^+ equilibrium potential will be ¨ 94 mV. This is close to the resting membrane potential of many excitable cells and indicates that the resting permeability is primarily determined by K^+-selective channels. This is true in muscle cells and in glial cells. However, resting channels in neurons are selective for several ion species including Na^+, Cl^- as well as K^+, thus the membrane potential, a balance of these permeable ions, is around ¨ 60 mV. The membrane potential at which no net current flows can be estimated from Goldman-Hodgkin-Katz voltage equation. Because the neuronal membranes at rest are more permeable to K^+ than to Na^+, the resting membrane potential is far from the Na^+ equilibrium potential (+55 mV) and is only slightly more positive than the equilibrium potential for K^+ (-85 mV).

For a neuron that has both a membrane voltage and K^+ concentration gradient, the K^+ current is estimated by the ohmic relation:

$$I_k = G_k (V_m - E_k)$$

Where G_k is the channel conductance, simply a reciprocal of resistance. V_m is the voltage across the membrane. This equation is a modified form of Ohm's law that takes into account that ionic current flow through a membrane is determined

not only by the voltage across the membrane but also by the ionic concentration gradients. The term (V_m ¨ Œ$_k$) is called the electrochemical driving force. The electrochemical driving force determines the direction of ionic current flow and along with the conductance, the magnitude of current flow.

Information is carried within and between neurons by electrical and chemical signals. Transient electrical signals are particularly important for carrying time-sensitive information rapidly and over long distances. These electrical signals are all produced by temporary changes in the current flow into and out of the cell that drive the electrical potential across the cell membrane away from its resting value. (Hille, 1992; Kandel, Schartz and Jessel, 2000). This current flow is controlled by ion channels in the cell membrane. There are two types of ion channels: resting and gated, which have distinctive roles in neuronal signaling. Resting channels normally are open and are not influenced significantly by extrinsic factors. They are primarily important in maintaining the resting membrane potential, the electrical potential across the membrane in the absence of signaling. Most gated channels, in contrast, are closed when the membrane is at rest. Their probability of opening is regulated by several factors: changes in membrane potential, ligand binding, or membrane stretch, etc.

The lipid bilayer of the membrane blocks the diffusion of ions, and an excitable cell has an excess of positive charges on the outside of the membrane and an excess of negative charges on the inside. The charge separation gives rise to a difference of electrical potential, or voltage, across the membrane. The resting membrane potential is the membrane potential of a cell at rest. A change in membrane potential to a more positive value is known as depolarization; hyperpolarization is a change to more negative potentials. When depolarization approaches a critical level, the threshold, the cell responds actively with the opening of voltage-gated ion channels, which at threshold produces an all-or-none action potential.

In the nerve cell at rest, the membrane potential is constant. There is no net current flow because the steady Na^+ influx equals to steady K^+ efflux. This balance changes, however, when the membrane is depolarized past the threshold for generating an action potential. Once the membrane potential reaches this threshold, voltage-gated Na^+ channels open rapidly. This regenerative, positive feedback cycle develops explosively, driving the membrane potential toward the Na^+ equilibrium potential of +55 mV.

The Na^+ permeability of the axon membrane rises rapidly and then decays during a step depolarization. Hodgkin and Huxley (1952a, b and c) said that g_{Na} activates and

inactivates. In the Hodgkin and Huxley analysis, activation is the rapid process that opens Na^+ channels during a depolarization. Inactivation is a slower process that blocks Na^+ channels following depolarization. Once Na^+ channels have been inactivated, the membrane must be repolarized or hyperpolarized to remove the inactivation. The inactivation process blocks the tendency of the activation process to open channels. Thus inactivation is distinguished from activation in its kinetics, which are slower, and in its effect, which is to close rather than to open channels during a depolarization. The Hodgkin-Huxley model describes permeability changes and predicts action potentials.

Voltage-gated ion channels respond to changes in the electric field across the membrane by undergoing conformational changes that open an ion permeable pore. The voltage dependence in the activation process is caused by the rearrangement of charges within the channel protein associated with some of the conformational transitions. These intramolecular charge movements can be directly measured as gating currents (Armstrong, 1981; Bezanilla, 1985). The molecular mechanisms of the conformational changes involved in channel gating have been studied extensively, particularly using cDNA clones of a number of different voltage-dependent ion channels, including voltage-dependent Na^+ channels (Catterall, 1992), Ca^{2+} channels (Tsien, Ellinor and Horne, 1991), and K^+ channels (Salkoff, Baker, Butler, Covarrubias, Pak and Wei, 1992; Hoshi and Zagotta, 1993).

II. Structure and function of voltage-gated Na^+ and Ca^{2+} channel α-subunits

The amino acid sequence of the voltage-dependent Na^+ and Ca^{2+} channels contains four homologous repeats. Hydropathy analysis suggests that each of these repeats contains six putative transmembrane segments (typically labeled S1-S6) (Fig. 2).

The S4 transmembrane segment in each motif is a region that contains a positively charged residue, arginine or lysine, spaced every third amino acid with intervening hydrophobic residues. This structure repeats several times to form an amphipathic helix (Noda, Shimizu, Tanabe, Takai, Kayano, Ikeda, Takahashi, Nakayama, Kanaoka, Minamino, Kahugawa, Matsuo, Raftery, Hirose, Inayama, Hayashida, Miyata and Numa, 1984). This region has been proposed to span the membrane and represent the voltage sensor for the voltage-dependent transitions (Greenblatt, Blatt and Montal, 1985; Catterall, 1986). The idea that the positive charges in the S4 region acts as the voltage sensor is supported by the fact that the S4 segment is found in most voltage-sensitive cation-selective channels so far cloned, and that its primary sequence is highly conserved.

In support of this idea, mutations of the S4 segment have been shown to alter the voltage sensitivity of a number of different channel types (Stuhmer, Conti, Suzuki,

Wang, Noda, Yahagi, Kubo and Numa 1989; Lopez, Jan, Jan 1991; Papazian, Timpe, Jan and Jan 1991). Such studies have shown that a reduction in the net positive charge in the S4 segment, produced by replacing positive charges with neutral or negatively-charged ones, leads to a decrease in the steepness of the voltage-dependence of activation (Stuhmer, Conti, Suzuki, Wang, Noda, Yahagi, Kubo and Numa 1989). There is evidence that 2 charged S4 residues move completely from an internally accessible to an externally accessible location in response to depolarization by passage through a short "channel" in the protein. This evidence comes from experiments in which each of the charged residues in the S4 domain was replaced by a cysteine (Yang, George and Horn 1996). The outmost basic residue of S4/D4, when changed from arginine to cysteine (D4:R1C), is accessible to extracellular application of the methanethiosulfonate (MTS) reagents methanethiosulfonate-ethyltrimethylammonium (MTSET) and " ethylsulfonate (MTSES) only when the channel is depolarized. The reaction of MTS reagents with the introduced cysteine residue was monitored by following changes in gating kinetics. This study has revealed that the S4 domain moves from the inside to the outside of the membrane in response to depolarization exposing two positive charges that were previously buried in the membrane as it does so.

The P loop between S5 and S6 forms part of the ion channel pore along with S6 and the cytoplasmic loop connecting S4 and S5, and this pore region determines the

single-channel conductance and ion selectivity.

III. Structure and function of voltage-gated K^+ channel α-subunits

Voltage-gated K^+ channels constitute a family of highly related proteins that are involved in a wide variety of biological processes including modulating electrical signals in neuron and muscle (Hille, 1992). They share significant similarities with voltage-gated Na^+ and Ca^{2+} channels; the genes that encode these cation channels are evolutionarily related and form a large gene family (Fig. 2).

A fascinating neurobehavioral phenotype consisting of jerking leg movements was noted in *Drosophila* when anaesthetized with ether. The phenotype was fittingly named *Shaker*. Physiological studies of *Drosophila* muscle cells revealed abnormalities in a rapidly inactivating K^+ current that led to the hypothesis that the *Shaker* locus is a K^+ channel gene. Since the cloning and molecular characterization of the first K^+ channel gene (*Shaker*) in 1987 (Tempel, Papazian, Schwarz, Jan, Jan, 1987; Papazian, Schwarz, Tempel, Jan, and Jan, 1987), a large number of K^+ channel genes have been identified. Following the identification of *Shaker*, a family of related channels was subsequently cloned from *Drosophila*, known as *Shab*, *Shaw* and *Shal*. Their mammalian counterparts are referred to as Kv1 (*Shaker*), Kv2 (*Shab*), Kv3 (*Shaw*) and Kv4 (*Shal*) (Dolly and Parcej, 1996; Wei, Jegla and Salkoff,

1996). At the amino acid level, there is about 70% homology within, and 40% homology between, the different subfamilies.

IV. Two types of inactivation in *Shaker* K^+ channels

Kv channels display two main modes of inactivation: fast and slow. The cytoplasmic amino terminus of the *Shaker* channel is responsible for its fast voltage-independent inactivation, which is therefore called N-type inactivation. Fast inactivating Kv currents are also known as A-currents.

N-type inactivation is a rapid inactivation that is voltage-independent and coupled to the activation processes. It has been shown to involve the intracellular region of the amino-terminal acting as a blocker of the pore, "ball and chain" type mechanism (Zagotta, Hoshi and Aldrich, 1989, 1990; Hoshi, Zagotta and Aldrich, 1990). Fast inactivation of Kv channels, like that of voltage-gated Na^+ channels, results from occlusion of the inner mouth of the pore by part of the channel protein. In the case of *Shaker* channels, the culprit is the cytosolic N terminus of the channel. The most distal part of this region serves as an inactivation "ball", which can swing into the channel pore and block ion fluxes, while the more proximal region acts as a "chain" which tethers the "ball" to the channel.

Kv channels also show an additional form of inactivation which is known as C-type inactivation. C-type inactivation is a slow inactivation which is independent of voltage over a range of ¨ Œ5 to +50 mV and seems to occur by a mechanism distinctly different from that determining N-type inactivation. It does not require intact N-type inactivation, but is partially coupled to it (Hoshi, Zagotta and Aldrich, 1991). It now appears that it involves residues at the outer mouth of the pore. It is believed that C-type inactivation involves a local conformational change at the external mouth of the pore which leads to constriction and occlusion of the pore (Liu, Jurman and Yellen, 1996).

V. Kv channels are made up of four subunits

K^+ channel α subunit proteins from the *Shaker* family contain six hydrophobic domains (S1-S6) that are thought to form amphipathic transmembrane helices (Fig. 2). However, the amino acid sequence of most voltage-gated K^+ channels, such as the *Shaker* channel cloned from *Drosophila*, is only approximately one fourth as long as those of voltage-gated Na^+ and Ca^{2+} channels and contains only a single S4 segment (Kamb, Tseng, and Tanouye, 1988; Pongs, Kecskemethy, Muller, Krah, Baumann, Kiltz, Canal, Llamazares, and Ferrus, 1988). Based on its sequence similarity to voltage-dependent Na^+ and Ca^{2+} channels, the *Shaker* K^+ channel is thought and has been proven to function as a tetramer of four *Shaker* subunits. In

support of this idea, MacKinnon (1991) has shown that block by scorpion toxin of heteromultimeric *Shaker* K^+ channels, formed by different proportions of toxin-sensitive and toxin-insensitive subunits, is consistent with a tetrameric structure. Furthermore, the block of the external pore by tetraethylammonium (TEA) has been shown to involve cooperative binding of TEA by all four subunits (Heginbotham and MacKinnon, 1992; Kavanugh, Hurst, Yakel, Varnum, Adelman and North, 1992; Liman, Tytgat and Hess, 1992). Direct evidence that the voltage-gated Kv channel is made up of 4 subunits subsequently came from studies carried out by Li and colleagues (Li, Unwin, Stauffer, Jan and Jan, 1994). They took the purified *Shaker* K^+ channel protein and imaged it using the electron microscope. The protein under the electron microscope is approximately square in outline, with a central hole that probably corresponds to the pore. In some images, the *Shaker* protein appeared to be partially dissociated and 4 globular domains, each of which presumably corresponds to a single subunit, could be clearly resolved.

VI. Kv channels can form homo-oligomers as well as hetero-oligomers

1. Electrophysiological Recordings from *Xenopus* Oocytes

A major goal of electrophysiology is to understand, at a molecular level, how an ion channel functions. Following the key observation of Gurdon, et al (Gurdon, Lane,

Woodland and Marbaix, 1971) that foreign RNA injected into oocytes could be translated into proteins, Gundersen and colleagues (Gundersen, Miledi and Parker, 1983) were the first to demonstrate that a variety of receptors and channels from the central nervous system could be functionally expressed in the oocyte. The recent dramatic advances in both molecular biology, where proteins can be routinely cloned and mutated at specific loci, and electrophysiology have combined to produce a powerful approach to the study of ion channels.

The oocytes do not contain an appreciable level of endogenous voltage-gated channels (the major one being a Ca^{2+}-activated Cl^- channel). Virtually all of the ionic and gating current arises from *Shaker* channels. By varying amount of RNA injected into the oocyte, we can record single-channel currents, macroscopic currents, and gating currents all in cell-free patches in the same preparation.

2. Kv channels can form homo-oligomers as well as hetero-oligomers

The subunits of the tetramer may be the same, generating homomeric channels, or in some cases different subunits may associate giving rise to heteromeric channels (Ruppersberg, Schroter, Sakmann, Stocker, Sewing, and Pongs, 1990; Christie, North, Osborne, Douglass, and Adelman, 1990). The presence of multiple subunits in K^+ channel proteins suggests a possible physical mechanism for the multiple

conformational changes occurring during activation. Opening of the channel might require separate conformational changes to occur in some or all of the subunits. This type of mechanism is typified by the model of Hodgkin and Huxley (Hodgkin and Huxley, 1952a, b and c) for the activation of squid voltage-dependent K^+ channels that involved the movement of four independent and identical gating particles.

Clearly, when *Xenopus* oocytes are injected with mRNA encoding a single type of subunit the Kv channel expressed must be homomeric. The fact that coinjection of oocytes with mRNAs encoding two different types of subunit may give rise to currents with hybrid properties indicates that heteromeric channels can be formed.

VII. Inactivation properties of voltage-gated K^+ channels are altered by the presence of β-subunits

According to the functional properties, voltage-gated K^+ channels (Kv) are roughly classified as delayed rectifier and A-type channels. Once open, delayed rectifier channels inactivate very slowly, while A-type channels activate at more hyperpolarized voltages and undergo rapid inactivation (Hagiwara, Kusano and Saito, 1961; Connor and Stevens, 1971a, b, c). On a molecular level, A-type currents can be attributed to voltage-gated channel α-subunits, which give rise to the N-type inactivation (Hoshi, Zagotta and Aldrich, 1990). From mammalian brain,

several α-subunits, such as Kv1.4, Kv3.4 and the Kv4 family, with A-type characteristics have been cloned (Stuhmer, Ruppersberg, Schroter, Sakmann, Stocker, Giese, Perschke, Baumann and Pongs, 1989; Schroter, Ruppersberg, Wunder, Rettig, Stocker and Pongs, 1991; Pak, Baker, Covarrubias, Butler, Ratcliffe and Salkoff, 1991). The majority of cloned Kv channel α-subunits, however, gives rise to currents of the delayed rectifier type.

Structure and functional diversity of voltage-gated Kv1-type K^+ channels is enhanced by the association of two different types of subunits, the membrane-bound, pore-forming α-subunit and the peripheral β-subunit. At least 3 different Kv β-subunit genes have been identified, and further diversity is generated by alternative splicing (Parcej, Scott and Dolly, 1992). There is no sequence homology between Kv channel β-subunit and those of Na^+ or Ca^{2+} channels. Coexpression of the predominant β subunit isoform in brain, Kvβ2, with a Kv1.2α subunit promotes cotranslational N-linked glycosylation of the nascent Kv1.2 polypeptide, increased stability of Kvβ2/Kv1.2 complexes, and increased efficiency of cell surface expression of Kv1.2 (Shi, Nakahira, Hammond, Rhodes, Schechter and Trimmer 1996). Association of Kvβ1 subunits with α-subunits also confers rapid A-type inactivation on non-inactivating Kv1 channels (Rettig, Helnemann, Wunder, Lorra, Parcej, Dolly and Pongs, 1994). Biochemical analysis showed a tight association of

α and β Kv channel subunits in 1:1 ratio, thus Kv channels which co-assemble with Kvβ-subunits constitute of four α- and four β-subunits. Therefore it was proposed that Kvβ subunits would contribute four N-terminal "ball" domains for inactivation of the delayed rectifier (Heinemann, Rettig, Graack and Pongs, 1996).

VIII. K^+ channel gating

1. Properties of single-channel currents

A single-channel current is recorded from a very small patch of membrane that contains only one channel using the patch clamp method. After a variable length of time, the channel initially opens and then closes. The length of time the channel remains open or closed is not constant but instead varies statistically depending on the structural configuration of the channel. For this reason, it is important to determine the mean open time and mean closed time by measuring the duration of a large number of openings and closings. The mean open time or mean closed time can be obtained from the open-time or closed time histogram, respectively, and is the time at which the number of events falls to 1/e of its maximal value. The open probability of the channel is defined as the fraction of time the channel spends in the open state and can be obtained by dividing the sum of all the open times by the duration of the recording. The amplitude of the current that flows when the channel

is open is constant. The channel is therefore said to have a single conductance state, i.e., it is either open or closed. The magnitude of the single-channel current is determined by the conductance of the channel and the potential across the membrane.

If the ion concentrations on either side of the membrane are not very different, then Ohm's law can be used to describe the current through the channel:

$i = V/R$ or $i = gV$

Where i is the single-channel current (in amps), V is the voltage gradient across the membrane (in Volts), the R is the resistance to current flow through the open channel (in Ohms), and the g is the single-channel conductance, simply the reciprocal of resistance. The linear relationship between membrane potential and the single-channel current amplitude follows Ohm's law.

When the ion concentrations on the inside and outside of the membranes are very different, the single-channel current-voltage relationship becomes

$i_k = g_k (V_m$ ¨ Œ$_k)$

Where V_m is the voltage across the membrane, E_k is the equilibrium potential for K^+, which can be calculated from Nernst equation. The net driving force on K^+ ions is now V_m ¨ Œ$_k$.

2. Boltzmann distribution

In a 2 state system, a particle spends less time in state of higher energy than in state of lower energy. It is defined by the Boltzmann equation, which gives relative probabilities at equilibrium of finding a particle in state 1 or state 2 if the energy difference between these states is u_2-u_1:

$$p_2/p_1 = \exp(-(u_2-u_1)/kT)$$

Where k is Boltzmann' s constant and T is absolute temperature on the Kelvin scale.

Another way of writing the Boltzmann equation is

$$P_o = \frac{1}{1 + \exp[-(V-V_{1/2})\, zF/RT]}$$

Where $V_{1/2}$ is the voltage at which half the channels are open, z is the valency of the

ion, R is the gas constant, T is the absolute temperature and F is the Faraday constant. This equation conveniently describes the equilibrium distribution of particles in force fields.

3. Gating current and gating current analysis

Gating current, denoted as Ig, arises from charge movements or dipole reorientations that accompany the conformational transitions of voltage-gated ion channels and are directly responsible for their voltage sensitivity. The study of gating currents provides valuable information about the mechanisms by which ion channels are controlled by voltage.

Gating currents are much smaller than ionic currents and it was some years before electronic techniques were good enough for them to be measured (Armstrong and Bezanilla, 1973; Keynes and Rojas, 1974). The gating current recordings require high channel densities, and low-noise performance at sufficiently high time resolution (Heinemann, Conti and Stuhmer, 1992). In order to demonstrate gating currents it is necessary to block the ionic currents with suitable agents, such as tetrodotoxin (TTX) for the Na^+ channels and tetramethylammonium (TEA) for the K^+ channels. This leaves just the gating currents and the current associated with the membrane capacitance. The capacitative current can be eliminated by algebraically

summing the current from exactly matched pulses of opposite sign. The remaining current is not symmetrical for pulses of opposite sign, and is gating current.

4. Kinetic analysis of single-channel currents

The kinetics of channel opening and closing provides information about the rates of transition between the closed and open states. The aim of a kinetic analysis is to describe the time course of the changes in channel properties in the hope that this will lead to ideas about their mechanism. Consider one simple possible model in which a channel can exist in only two states: open (O) or closed (C). The kinetic behavior of this channel is given by

$$\text{(closed) C} \underset{k_{-1}}{\overset{k_1}{\rightleftharpoons}} \text{O (open)}$$

Where k_1 and k_{-1} are the rate constants (in sec^{-1}) for entering and leaving the open state, respectively. The time spent in any one state is given by the reciprocal of the sum of the rate constants for leaving that state. Thus the mean open time is simply $1/k_{-1}$ and the mean closed time is $1/k_1$. The rate constants may therefore easily be obtained by measuring the mean open and closed times. With a single open (or

closed) state, the open (or closed) time distribution will follow a single exponential and the mean open (or closed) time will be given by the time constant of the distribution.

For a voltage-independent channel, the rate constants will be unaffected by membrane potential. In the case of a voltage-dependent channel, the mean open and closed times vary with membrane potential, and the open probability is also voltage dependent. In many cases, ion channels have more than one closed state, so that the channel may pass through additional states during its transition from the resting to fully open state.

Studies on the kinetics of voltage-dependent *Shaker* K^+ channels have identified a number of general properties of the gating mechanism (Hoshi, Zagotta and Aldrich, 1994; Zagotta, Hoshi, Dittman and Aldrich, 1994; Zagotta, Hoshi and Aldrich, 1994; Schoppa and Sigworth, 1998a, b and c). Comparison of the time to first opening (the single-channel first latency) distribution and the time course of the ensemble average current for voltage-dependent *Shaker* K^+ channels showed that the activation time course and its voltage dependence are largely determined by the transitions before first opening. The open dwell time data are consistent with a single kinetically distinguishable open state. Once the channel opens, it can enter at least two closed states which are not traversed frequently during the activation process. The rate

constants for the transitions among these closed states and the open state are nearly voltage-independent at depolarized voltages (>-30 mV) (Hoshi, Zagotta and Aldrich, 1994).

Voltage-dependent gating behavior of *Shaker* K^+ channels without N-type inactivation (ShB Δ 6-46) expressed in *Xenopus* oocytes indicated the activation process involves the movement of the equivalent of 12-16 electronic charges across the membrane and the results were generally consistent with models involving a number of independent and identical transitions with a major exception that the first closing transition is slower than expected (Zagotta, Hoshi, Dittman and Aldrich, 1994).

5. Macroscopic currents

The macroscopic current (I) represents the summed current through all of the channels in a patch of membrane. It is related to the single-channel current (i) in the following way:

$$I = N P_o i$$

Where P_o is the channel open probability and N is the number of channels in the

membrane. In response to depolarization, the macroscopic current increases slowly after a delay and gradually reaches a steady-state level. This slow turn-on of the current is known as activation. Because there is a time-dependent increase in the channel open probability and each channel opens at random, after summing up all the single-channel currents, the activation phase of the macroscopic current can be plotted as a smooth curve.

Due to the voltage-dependent increase in P_o, the macroscopic current-voltage relation differs from that of the single-channel. The magnitude of the macroscopic current is determined both by the single-channel current amplitude, and by the channel open probability.

EA-1 Mutations in Kv1.1 Alter K^+ Channel Function by Dominant Negative Effects and Haploinsufficiency

The positions of the amino acids in Kv1.1 that have been linked to EA-1 are shown in Fig. 1. The different locations of the various EA-1 point missense mutations suggest that they may affect distinct aspects of voltage-gated K^+ channels. Furthermore, they occur at positions that are highly conserved among the voltage-dependent K^+ channels.

The Adelman and Maylie group (Adelman, Bond, Pessia, and Maylie, 1995) first incorporated the EA-1 mutations into the Kv1.1 and found that some of the EA-1 alleles encode functional channels in *Xenopus* oocytes, which had been injected with EA-1 cRNAs. EA-1 subunits formed functional homomeric channels with lower current amplitudes and altered gating properties compared with wild type subunits. Further study demonstrated that two EA-1 subunits in the first cytoplasmic loop, R239S and F249I, has no current in the two-electrode voltage-clamp recordings and show very low protein yield in the Western plot analysis, which may suggest that these two EA-1 mutations result in unstable subunits and may affect the symptoms of EA-1 by haploinsufficiency. The absence or marked reduction of currents for R239S and F249I subunits, respectively, together with reduced amounts of protein, suggest that the intracellular loop between transmembrane domains 2 and 3 is critical for channel biosynthesis and subunit stability (Zerr, Adelman and Maylie, 1998).

EA-1 is an autosomal dominant disease, and all known individuals are heterozygous. If both EA-1 and wild-type Kv1.1 alleles are expressed to a similar extent *in vivo*, the EA-1 and wild-type subunits may assemble according to a binomial distribution (MacKinnon, 1991; Kavanugh, Hurst, Yakel, Varnum, Adelman and North, 1992). Therefore, when equal amounts of EA-1 mutations and wild type cRNAs were coinjected, mimicking the heterozygous condition, it resulted in current amplitudes and gating properties that were intermediate between wild-type and EA-1

homomeric channels, suggesting that heteromeric channels are formed with a mixed stoichiometry of EA-1 and wild-type subunits, and that EA-1 mutations in Kv1.1 alter K^+ channel function. To examine the relative contribution of EA-1 subunits in forming heteromeric EA-1 and wild type channels, each EA-1 subunit was made insensitive to TEA (TEA tagged) by substitution of valine for tyrosine (Y379V) which reduces sensitivity to TEA about 100-fold. The results showed that heteromeric channels are formed from an equal amount of wild type and EA-1 subunits (Zerr, Adelman and Maylie, 1998). This was first time ever in which coinjection was studied.

Two EA-1 mutations (E325D and V408A) each forms functional homomeric channels with accelerated activation, faster deactivation, increased C-type inactivation and lower current amplitude compared with wild type (Adelman, Bond, Pessia, and Maylie, 1995; Zerr, Adelman and Maylie, 1998). V408A channels have voltage dependence similar to that of wild type channels, but with faster kinetics and increased C-type inactivation (Fig. 3). Measured at 40 mV, V408A subunits have only half the current amplitude of the wild type. The activation kinetics of V408A channels are best described by a double exponential function. V408A channels activate approximately 2- to 3- fold faster than wild type channels. Deactivation is 10-fold faster for V408A channels than for wild type at all voltages and is more voltage dependent. Both V408A and wild type channels clearly undergo C-type

inactivation; however, the rate of C-type inactivation is 7-fold faster for V408A compared with the wild type. Similar to V408A channels, the activation and deactivation of E325D are 6-fold faster compared with wild type (Fig. 4). C-type inactivation is faster than for wild type, too, yielding an increased amount of inactivation. But the current amplitude is much smaller for E325D, only 3.8% of the wild type. Additionally, the voltage dependence of E325D channels was shifted about 60 mV positively.

Objectives

Previous two-electrode voltage-clamp studies showed that V408A and E325D subunits formed functional homomeric channels with lower macroscopic current amplitude, and altered gating properties compared with wild type (Adelman, Bond, Pessia and Maylie, 1995; Zerr, Adelman and Maylie, 1998).

Macroscopic current (I) represents the summed current through all of the channels in a patch of membrane. It is related to the single-channel current (i) in the following way:

$$I = N P_o i$$

$i = g_k (V_m - E_k)$

Where P_o is the channel open probability, N is the number of channels in the membrane and g_k is the single-channel conductance. It is clear that several factors could change the macroscopic current (I): number of channels (N) in the patch, channel open probability (P_o). In addition, a change in single-channel conductance (g_k) could alter single-channel current (i).

We focused our attention on mutations E325D and V408A. They reside on the both sides of the P loop: E325D at the cytoplasmic interface of S5, and V408A in the C-terminal portion of S6. The E325D and V408A mutations are remarkable because they show interesting kinetics in the previous two-electrode voltage-clamp study. Since previous work has found that these two mutations have lower current amplitude, increased rate of activation, accelerated C-type inactivation and deactivation, further understanding of the mechanisms at the single-channel level is crucial.

Since previous two-electrode voltage-clamp recordings showed that V408A and E325D subunits formed functional homomeric channels with lower current amplitude and altered gating properties compared with wild-type, we investigated the EA-1 subunit gating mechanism at the single-channel level, and utilized single-

channel recordings to analyze the single-channel conductance and channel open probability. The analysis of the single-channel currents also provides a direct estimate of the number of open and closed conformations entered after the first opening and of the rate and voltage-dependence of the transitions between these conformations. From these data, we could predict the kinetics and the mechanisms of the EA-1 mutations at the single-channel level.

Materials and Methods

Channel Expression

Human Kv1.1 cDNA was cloned into the vector pS$^-$, derived from pSelect plasmid (Promega, Madison, WI). All *in vitro* transcription properties of pS$^-$ are identical to those of pSelect. Human Kv1.1 was the generous gift of Dr. Mark Tanouye and was cloned in the vector pSK. Each mutant was introduced into the Kv1.1 by site-directed mutagenesis as made before (Adelman, Bond, Pessia, and Maylie, 1995). The complete nucleotide sequences of the coding regions for all expression plasmids including wild type hKv1.1 and the two EA-1 mutations, E325D and V408A, were verified prior to RNA synthesis and injection. Nucleotide and protein sequence computer analysis was performed using Genetics Computer Group software. Equal amounts of cDNA were linearized and

transcribed into cRNA for later injection. cRNA was initially evaluated by denaturing gel electrophoresis and ethidium bromide stain as well as by spectrophotometer. All molecular biology enzymes were purchased from BRL. Oligonucleotides were purchased from Genosys.

Human Kv1.1 wild type and the two EA-1 mutations, E325D and V408A, were expressed in *Xenopus* oocytes by injecting cRNA as described previously (Adelman, Bond, Pessia, and Maylie, 1995). *Xenopus* frogs were handled in accordance with the institutional guidelines and underwent no more than two surgeries separated by at least three weeks. To isolate oocytes, frogs were anesthetized with an aerated solution of 3-aminobenzoic acid ethyl ester. Standard techniques were practiced during *in vitro* cRNA synthesis, and oocyte handling and injection (Adelman, Shen, Kavanaugh, Warren, Wu, Lagrutta, Bond, and North, 1992). After injection, the oocytes were incubated at 16 °C in ND96 medium of the following composition (mM): 96 NaCl, 2 KCl, 1.8 $CaCl_2$, 1 $MgCl_2$, 5 HEPES, 2.5 NaPyruate, 0.5 Theophylline, 50 μg/ml Gentamycin, pH 7.4. Current measurements were made 2-7 d after injection with 2 ng of cRNA.

Measurement of Single-Channel Ionic Currents

Single-channel recordings from the expressed channels were made using the cell-

free inside-out patch-clamp method (Hamill, Marty, Neher, Sakmann, and Sigworth, 1981). Oocytes were devitellinized immediately prior to patch-clamp recording. Patch electrodes were pulled from borosilicate glass with a tip resistance of 10-20 MΩ, coated with Sylgard, and fire polished before use. Membrane patches were voltage clamped with an Axopatch 200A amplifier using a CV 201A headstage (Axon Instruments, Foster City, CA). Recordings were stored directly on Macintosh Quadra 650 computer. All experiments were performed at room temperature.

Data Analysis

Single-channel recordings were analyzed with MacTac (Bruxton Corp., Seattle, WA) using the standard "50% threshold" technique to estimate event amplitudes and duration, and each transition was visually inspected before being accepted. Leak subtraction was performed by subtracting an average of 8-20 sweeps of the null traces (no single-channel openings) to get rid of leak and capacitance artifact. Open- and closed" duration histograms were constructed using MacTacfit (Bruxton Corp.). The open and closed durations were fitted with sums of exponential probability density functions (pdf' s) using the maximum likelihood method with simplex optimization. A histogram is displayed as an approximation to the pdf by counting the number of observations that fall in

intervals (bins) of specified width. Open and closed duration histogram are shown using the log-binning transformation of Sine and Sigworth (Sigworth and Sine, 1987). The number of exponential components present in a data set was determined using the likelihood ratio test (Kalbfleish, 1985).

A correction was made for the rise time of the filter (Colquhoun and Sigworth, 1983) and all bins were used for fitting. The number of channels present in a patch was determined by observing the maximum number of channels open simultaneously at voltages where the probability of channel being open was high. Only the data from single-channel patches are used. The number of statistically significant components was determined by using the method of maximum likelihood ratios (Horn and Lange, 1983). Missed events were not corrected. Values were expressed as mean $\pm$ SEM. Results were considered significantly different at $P < 0.01$.

Solutions

During recording, oocytes were bathed in a solution containing (mM): 120 KCl, 5 NaCl, 10 HEPES and 5 EGTA and djusted to pH 7.2 with KOH. Electrodes were filled with a solution containing (mM): 125 NaCl, 10 HEPES, pH 7.2. All chemicals were from Sigma (St. Louis, MO)

RESULTS

Recordings of Single-Channel Ionic Currents

Representative single-channel current traces of the wild type, V408A and E325D elicited in response to 200 ms depolarizing voltage pulses to different potentials from a holding potential of ¨ 80 mV are shown in Figure 5. All three channels reveal a latency to first opening (delay between vertical dashed line and first opening) that appears to decrease with increasing voltage. Wild type channels do not enter a long duration closed state after opening consistent with the lack of N-type inactivation and minimal C-type inactivation. However, some of the traces from V408A and E325D reveal a long closed state after opening that may reflect the faster C-type inactivation for these mutations. Further, comparison of the traces at similar depolarizing voltages reveal that after opening V408A and E325D flicker between open and closed state more often than wild type indicative of a destabilized open state.

Single-Channel Conductance of V408A and E325D

Figure 6 shows that wild type, V408A and E325D channels enter a single

conductance state within the time course of the recordings. Single channel currents were determined from an all point histogram at each voltage and plotted versus membrane potential (Fig. 6). For comparison a line with a slope conductance of 10.5 pS was drawn on the graph. The single-channel conductance (pS) for wild type, E325D and V408A channels were 10.5±0.459 (n=5), 10.5±0.786 (n=3) and 10.0±0.577 (n=3), respectively. The F value of one way analysis of variance (ANOVA) is 0.199 and the P value is 0.824 (>0.001). This result shows that the EA-1 mutations, V408A and E325D, do not affect the single channel conductance and that the reduction in whole cell current observed with these EA-1 mutations is not the result of a decreased single channel conductance.

Behavior of Ensemble Currents

Ensemble traces were constructed from the average of all the sweeps at each depolarizing voltage (Fig. 7A). The time course of the probability relaxation to steady state became more rapid and the probability the channel was open increased for depolarization from ¨ 60 to 20 mV. Moreover, the open probability did not exhibit a time-dependent decay suggesting that C-type inactivation does not compromise the data on this time scale. The steady-state open probability determined from all patches was averaged and plotted as a function of voltage (Fig. 7B). The data were fitted with a single Boltzmann distribution yielding the

results shown in Table 2. The voltage at which half the channels were open, $V_{1/2}$, was -42 mV for wild type and -43 mV for V408A. The mutation E325D shifted the $V_{1/2}$ to -26 mV and reduced the steepness factor from 4 to 10 mV consistent with, but not as dramatic as, that determined from the whole oocyte using two-electrode voltage clamp.

Table 2. Parameters from Boltzmann fit to ensemble probability

	P_{max}	$V_{1/2}$ (mV)	k (mV)	N
WT	0.75	-42.2	4.1	5
V408A	0.53	-43.3	5.3	3
E325D	0.52	-26.2	10.2	3

First Latency Distribution

In *Shaker* K^+ channel from *Drosophila*, it was shown that the first latency distribution and ensemble averages coincide with each other, which strongly support the idea that the activation time course and voltage dependence at depolarized voltages are determined by the transitions before first opening (Hoshi, Zagotta and Aldrich, 1994).

Figure 8A shows the cumulative distribution of first latencies for voltages between ¨ 60 and +20 mV. The distributions at some voltages are sigmoidal at depolarized voltages. This departure of the distribution from a single-exponential distribution is generally interpreted to indicate that the channel must progress

through multiple closed states, or undergo multiple conformational transitions, before opening. The first latency distributions saturate near a probability of 1 for the more depolarized voltages, indicating that only rarely did the voltage pulse fail to elicit openings.

Similar to the ensemble averages, the time course of the first latency distributions becomes more rapid as the voltage becomes more depolarized. A single exponential was applied to the rising phase of the first latency distributions and the average time constants were plotted as function of voltage (Fig. 8B). V408A had fastest first latency time constants, wild type had slowest, E325D in between. These results were consistent with two-electrode voltage-clamp study (Zerr, Adelman and Maylie, 1998; Adelman, Bond, Pessia and Maylie, 1995) which EA-1 mutations, V408A and E325D, have much faster activation than wild type.

Transitions After First Opening Are Voltage-Independent at Depolarized Voltages

A patch clamp record of the activity of a single channel will show a sequence of alternate open and shut periods of different durations. The duration of any particular open or closed event is called dwell time. A common method of analyzing single channel records is to sort the individual events according to their

dwell times, putting them into a series of bins of constant width. After closing or openings have been sorted in this way, a dwell time histogram for the closed state or open state of the channel, respectively, can be constructed.

The durations of the open and closed events elicited by steps to voltages between ¨ 60 and +50 mV were first analyzed in *Shaker* (Hoshi, Zagotta and Aldrich, 1994). This analysis of the single-channel gating kinetics predicts that the distribution of closed durations will be described by a sum of N exponential components where N represents the minimum number of closed states that the channel enters after opening. The maximum likelihood for 1 to 3 exponential components were compared by the likelihood ratio test to determine the number of significant components required to describe the distribution of closed durations. This analysis of the closed durations revealed the occurrence of three closed conformations after the channel first opened in *Shaker* (Hoshi, Zagotta and Aldrich, 1994).

Figure 9A plots the frequency distribution of closed events from wild type, V408A and E325D channels during steps to voltages at ¨ 40 mV, 0 mV and 20 mV. The distributions are plotted and fitted with the maximum likelihood estimates of distributions containing three exponential components. The time constants and amplitudes of each component from a number of different single-

channel patches of wild type (n=5), V408A (n=3) and E325D (n=3) are plotted as a function of voltage in Figure 9B.

Wild type and EA-1 mutations all have 3 components of closed duration time constants. There is no difference in any of the three components among wild type, V408A and E325D channels. The fast component, 0.3 ms in duration, can be seen as flicker closings in the single-channel records (Figure 5). These closings represent the most frequently observed closed events, over 70% of the closures. The duration and frequency of these events is only weakly dependent on voltage between ¨ 60 and +60 mV. In general, a one to one correspondence between a component of the closed time histogram and a discrete closed state can only be made when transitions between closed states do not occur. If the fast component arises primarily from a single closed conformation, this weak voltage dependence suggests that there is little charge movement associated with the reopening conformational change, between the closed conformation and the transition state to opening.

The intermediate component of the distribution of closed durations is 1 to 5 ms in duration and comprises about 30% of the closures. Its time constant and relative amplitude also display very little voltage dependence between ¨ 60 and +60 mV. The same argument as for the fast component applies; if this component arises

from a single closed conformation, this suggests that little charge movement occurs between the intermediate closed conformation and the transition state to reopening.

In contrast to the fast and intermediate components, the slow component is frequently not significant at depolarized voltages and is more prevalent in the activation voltage range, at ¨ 40 mV and ¨ 50 mV, than at the depolarized voltages.

E325D and V408A affect the open duration

The closing conformational changes can be studied by an analysis of the open durations. In *Shaker*, the open events elicited by steps to voltages between ¨ 50 and +50 mV were sufficiently described by a single exponential distribution and did not warrant a distribution containing two or more components. This suggests that only a single open conformation is kinetically distinguishable. This finding is true for wild type, V408A and E325D as well.

Figure 10A plots the frequency distribution of open durations from single patches of wild type, V408A and E325D, respectively. The distributions are fitted with the maximum likelihood estimate of a single exponential distribution.

Figure 10B plots the frequency distribution of open durations from all the patches of wild type, V408A and E325D as a function of voltage. Similar to *Shaker*, the mean open duration of wild type has no voltage dependence between ¨ 60 and +50 mV (Hoshi, Zagotta and Aldrich, 1994). However, the mean open duration of the two EA-1 mutations, E325D and V408A, was voltage dependent between ¨ 60 and +50 mV.

The open duration is governed by the rate constants of all of the closing conformational changes and is numerically equal to the reciprocal of the sum of all the closing rate constants. This sum is dominated by the most rapid closing rate constant. In *Shaker*, one model predicts that there are a number of independent and identical transitions with a major exception that the first closing transition is slower than expected and serves as the rate-limiting step (Zagotta, Hoshi, Dittman and Aldrich, 1994). Similar to that model, we predict that EA-1 mutations E325D and V408A affect the rate-limiting first closing transitions, and destabilize the open state.

DISCUSSION

EA-1 mutations, E325D and V408A, in human Kv1.1 have been examined for the differences of single-channel properties with wild type channels.

The E325D and V408A mutations were shown in a previous two-electrode voltage-clamp study, to form functional homomeric channels with lower current amplitude and altered gating properties as compared to wild type channels (Adelman, Bond, Pessia and Maylie, 1995; Zerr, Adelman and Maylie, 1998). Both showed accelerated activation and deactivation kinetics and faster C-type inactivation. Additionally, the E325D mutation shifted the voltage dependence positively by 60 mV, and both activation and deactivation kinetics were less steeply voltage dependent. The voltage dependence of activation as determined by a Boltzmann fit was also less steep.

In our single-channel analysis we have shown that EA-1 mutations E325D and V408A did not affect single channel conductance. The single channel conductance (pS) for wild type, E325D and V408A was 10.48 ± 0.459 (n=5), 10.467 ± 0.786 (n=3) and 10.00 ± 0.577 (n=3), respectively. This result indicates that the macroscopic current amplitude was not caused by a reduction in the channel conductance.

The most likely cause of lower current amplitude for E325D and V408A is a lower open probability. Lower current amplitude could also be caused by a lower number of channels expressed in the membrane, which we can not rule out from

our study. The open probability for V408A and E325D was one third lower than for the wild type. The probability increased steeply between ¨ 60 and ¨ 30 mV for wild type and V408A, and between ¨ 40 and ¨ 20 for E325D channels. The open probability saturated at about 0.75 above ¨ 30 mV for wild type, at 0.53 above ¨ 30 mV for V408A, and at 0.52 above ¨ 00 mV for E325D. This clearly shows that V408A and E325D channels had lower open probabilities than the wild type channels.

In the *Shaker* K^+ channel study (Hoshi, Zagotta and Aldrich, 1994), it was shown that the activation time course and voltage dependence at depolarized voltages are determined by the transitions before first opening. In our analysis, wild type channels had the slowest first latency time constant, which means they activated most slowly. V408A channels, on the other hand, had the fastest activation. E325D channels was in between. These results are consistent with previous two-electrode voltage-clamp studies (Adelman, Bond, Pessia and Maylie, 1995; Zerr, Adelman and Maylie, 1998).

Kv1.1 is a mammalian homolog of the *Shaker* K^+ channel (Tempel, Jan, and Jan, 1988; Baumann, Grupe, Ackermann, and Pongs, 1988). Multiexponential life-time distributions indicate the presence of multiple channel states. In our analysis, we have shown that there are at least three closed conformations in the

activation voltage range: a fast, intermediate and slow component consistent with what has been shown for the *Shaker* K^+ channel. The fast component contributed the largest percentage, 70% of the closures, with a mean closed time of 0.3 ms in duration. The intermediate component had a mean closed time of 1-3 ms and contributed 30% of the total closures. The slow component with a mean closed time of over 10 ms contributed a low percentage of the total closures, less than 10%. These results are similar to those described for the *Shaker* K^+ channel (Hoshi, Zagotta and Aldrich, 1994) and showed that Kv1.1 and *Shaker* K^+ channels share similar gating properties.

The closing conformational changes can be studied by an analysis of the open durations. Our study showed that only a single open conformation is kinetically distinguishable in the wild type, E325D and V408A. Similar to the *Shaker* K^+ channel (Hoshi, Zagotta, and Aldrich, 1994) we observed that the open time constant of the wild type was voltage independent; however, one striking discovery of the current study was that these two EA-1 mutations had a voltage dependent open time constants. In *Shaker*, one model predicts that there are a number of independent and identical transitions with a major exception that the first closing transition is slower than expected and serves as the rate-limiting step (Zagotta, Hoshi, Dittman and Aldrich, 1994). Similar to that model, we predict that EA-1 mutations E325D and V408A affect the rate-limiting first closing

transitions, and destabilize the open state.

Our data suggest that the overall macroscopic current and the kinetics of the mutation channels could be altered by the changes in single-channel properties. These results are consistent with a cellular model for EA-1 in which the delayed rectifier K^+ current does not efficiently repolarize the nerve cell following an action potential. Stress may alter the excitability of GABAergic cerebellar neurons expressing the voltage-gated delayed rectifier K channel Kv1.1. Kv1.1 is primarily localized in cerebellar interneurons thought to be GABAergic (Wang, Kunkel, Martin, Schwartzkroin, Tempel 1993; Wang, Kunkel, Martin, Schwartzkroin, Tempel 1994). The reduced delayed rectifier function prolongs the action potential and increases GABA release. The resulting increased GABA inhibitory input in the cerebellum offsets the balance between inhibitory and excitatory inputs. Increases in circulating catecholamines induced by physical exercise or stress increases inhibitory synaptic activity (Llano and Gerschenfeld, 1993), and may be the insult that further destabilizes motor control in EA individuals, resulting in ataxia. So, the clinical symptoms of EA-1 are the result of altered K channel function leading to abnormalities in the excitability of the peripheral and central nervous system.

Not all the macroscopic changes can be explained by the single-channel

properties. However, useful information may be obtained from comparing gating currents. Since gating currents can provide important information on the conformational changes when channels open or close, the comparison among the EA-1 mutations and wild type channels could help explain the mechanism of the accelerated deactivation by the EA-1 mutations. Preliminary data has been generated from non-conducting wild type channels by using cut-open oocyte technique (data not included). Higher expression than has been achieved so far will be necessary for V408A and E325D channels. Because of the lower open probability, V408A and E325D channels have large number of cells in the unopen state at depolarized voltages. The charges unlocked by the open state would be readily available, which would create a high peak and short duration OFF gating current.

The human genome contains more than 25 separate genes encoding Kv subunits. In many cases, Kv subunits which are closely related structurally also share common functional characteristics, suggesting that because of their fundamental importance, they may be redundant. However, EA-1 results from the smallest possible mutation, a single base change in only one Kv gene. Even in heterozygous arrangement, these mutations provoke clinical abnormalities, suggesting that each Kv gene encodes a subunit which performs a unique role. It is clear from EA-1 that Kv genes are not redundant, and each provides a particular

chord in the electrical symphony of the nervous system. These studies provide a good rational for the generation of transgenic mouse models for EA-1. A transgenic mouse would provide an animal model for the disease and a source of tissue to examine whether affected nerve cells display a prolonged action potential duration.

SUMMARY AND CONCLUSION

Subunits of the voltage-gated K^+ channel Kv1.1 containing mutations responsible for episodic ataxia type 1 (EA-1), an autosomal dominant neurological disorder, were expressed in *Xenopus* oocyte and their single-channel properties were studied. Single-channel recordings from the expressed channels were made using the cell-free inside-out patch-clamp method. Single-channel current analysis showed that two EA-1 mutations E325D and V408A decreased the channel open probability significantly, from 0.75 for wild type channels to 0.53 for V408A, and to 0.52 for E325D, but had no effect on single-channel conductance compared with wild type. The single-channel conductance (pS) for wild type, E325D and V408A was 10.48 ± 0.459 (n=5), 10.467 ± 0.786 (n=3) and 10.00 ± 0.577 (n=3), respectively ($P>0.01$). The first latency time constants at different voltages were compared between wild type and EA-1 mutations. V408A channels had fastest activation, wild type channels had slowest activation, E325D channels in

between. These results were consistent with a two-electrode voltage-clamp study (Adelman, Bond, Pessia and Maylie, 1995; Zerr, Adelman and Maylie, 1998) in which EA-1 mutations, V408A and E325D channels, had faster activation than wild type. Transitions after first opening are voltage-independent at depolarized voltages. Wild type and EA-1 mutations all have 3 components. There is no difference between wild type and V408A or E325D. The fast component, 0.3 ms in duration, can be seen as flicker closings in the single channel records. These closings represent the most frequently observed closed events, over 70% of the closures. The intermediate component of the distribution of closed durations is 1 to 5 ms in duration and comprises about 30% of the closures. In contrast to the fast and intermediate components, the slow component is frequently not significant at depolarized voltages and is more prevalent in the activation voltage range, at ¨ 40 mV and ¨ 60 mV, than at the depolarized voltages. In all patches the open events elicited by steps to voltages between ¨ 60 and +50 mV were sufficiently described by a single exponential distribution and did not warrant a distribution containing two components. This suggests that only a single open conformation is kinetically distinguishable in the wild type, E325D and V408A. More importantly, EA-1 mutations, E325D and V408A, decreased open time constants dramatically and caused the latter became voltage-dependent. Taken together, these results show that EA-1 mutations, E325D and V408A, decreased the open probability and destabilized open state.

REFERENCES

Adelman JP, Bond CT, Pessia M and Maylie J (1995). Episodic ataxia results from voltage-dependent K^+ channels with altered functions. *Neuron* 15: 1449-1454.

Adelman JP, Shen KZ, Kavanaugh MP, Warren RA, Wu YN, Lagrutta A, Bond CT, and North RA. (1992). Ca^{2+}-activated K^+ channels expressed from cloned complementary DNAs. *Neuron* 9:209-216.

Armstrong CM (1981). Na^+ channels and gating currents. *Physiological Review* 61: 644-683.

Armstrong CM and Bezanilla F (1973). Currents related to movement of the gating particles of the Na^+ channels. *Nature* 242: 459-461.

Ashcroft FM (2000). Ion Channels and Disease: channelopathies. Academic Press, San Diego, CA.

Baumann A, Grupe A, Ackermann A, and Pongs O (1988). Structure of the voltage-dependent K^+ channels is highly conserved from *Drosophila* to vertebrate central nervous systems. *EMBO J* 7: 2457-2463.

Bezanilla F (1985). Gating of Na^+ and K^+ channels. *J Membrane Biology* 88: 97-111.

Browne DL, Gancher ST, Nutt JG, Brunt ERP, Smith EA, Kramer P, and Litt M (1994). Episodic ataxia / myokymia syndrome is associated with point mutations in the human K^+ channel gene, KCNA1. *Nat Genet* 8: 136-140

Browne DL, Brunt ERP, Griggs RC, Nutt JG, Gancher ST, Smith EA, and Litt M (1995). Identification of two new KCNA1 mutations in episodic ataxia/myokymia families. *Hum Mol Genet* 4: 1671-1672

Brunt ER, and van Weerden TW (1990). Familial paroxysmal kinesiogenic ataxia and continuous myokymia. *Brain* 113: 1361-1382

Catterall WA (1986). Molecular properties of voltage-sensitive Na^+ channels. *Annual Review of Biochemistry* 55: 953-985.

Catterall WA (1992). Cellular and molecular biology of voltage-gated Na^+ channels. *Physiological Reviews* 72: s15-48.

Celesia GG (2001). Disorders of membrane channels or channelopathies. *Clinical Neurophysiology* 112: 2-18.

Christie MJ, Adelman JP, Douglass J, and North RA (1989). Expression of a cloned rat brain K^+ channel in *Xenopus* oocytes. *Science* 244: 221-224

Christie MJ, North RA, Osborne PB, Douglass J, and Adelman JP (1990). Heteropolymeric K^+ channels expressed in Xenopus oocytes from cloned subunits. *Neuron* 2: 405-411

Colquhoun D, and Sigworth FJ (1983). Fitting and statistical analysis of single-channel records. *In* Single-Channel Recording. Sakmann, B. and Neher, E., editors. Plenum Publishing Corp., New York. 191-263.

Connor JA and Stevens CF (1971a). Inward and delayed outward membrane currents in isolated neural somata under voltage clamp. *J Physiol* 213:1-19.

Connor JA and Stevens CF (1971b). Voltage clamp studies of a transient outward membrane current in gastropod neural somata. *J Physiol (London)* 213:21-30.

Connor JA and Stevens CF (1971c). Prediction of repetitive firing behavior from voltage clamp data on an isolated neurone soma. *J Physiol (London)* 213:31-53.

Cooper EC and Jan LY (1999). Ion channel genes and human neurological disease: recent progress, prospects, and challenges. *Proc Natl Acad Sci* 96: 4759-4766.

Doyle DA, Morais Cabral J, Pfuetzner RA, Kuo A, Gulbis JM, Cohen SL, Chait BT, MacKinnon R (1998). The structure of the potassium channel: molecular basis of K+ conduction and selectivity. *Science* 280: 69-77.

Dolly JO and Parcej DN (1996). Molecular properties of voltage-gated K^+ channels. *J Bioeng Biomembr* 28: 231-253.

Fontaine B, Khurana TS, Hoffman EP, Bruns GA, Haines JL, Trofatter JA, Hanson MP, Rich J, McFarlane H and Yasek DM (1990). Hyperkalemic periodic paralysis and the adult muscle Na^+ channel α-subunit gene. *Science* 250: 1000-1002.

Gancher ST, and Nutt JG (1986). Autosomal dominant episodic ataxia: a heterogeneous syndrome. *Mov Disord* 1: 239-253.

Greenblatt RE, Blatt Y, and Montal M (1985). The structure of the voltage-sensitive Na^+ channel. *FEBS Lett* 193: 125-134.

Griggs RC and Nutt JG (1995). Episodic ataxias as channelopathies. *Ann Neurology* 37: 285-287.

Gundersen CB, Miledi R and Parker I (1983). Serotonin receptors induced by exogenous messenger RNA in Xenopus oocytes. *Proc R Soc Lond B Biol Sci* 219: 103-109.

Gurdon JB, Lane CD, Woodland HR and Marbaix G (1971). Use of frog eggs and oocytes for the study of messenger RNA and its translation in living cells. *Nature* 233: 177-182.

Hagiwara S, Kusano K and Saito N (1961). Membrane changes of *Onchidium* nerve cell in K^+-rich medium. *J Physiol (London)* 155: 470-489.

Hamill OP, Marty A, Neher E, Sakmann B, and Sigworth FJ (1981). Improved patch-clamp techniques for high-resolution current recording from cells and cell-free membrane patches. *Pflugers Archiv*. 391: 85-100.

Heginbotham L and MacKinnon R (1992). The aromatic binding site for tetraethylammonium ion on K^+ channels. *Neuron* 8: 483-491.

Heinemann SH, Conti F and Stuhmer W (1992). Recording of gating currents from *Xenopus* oocytes and gating noise analysis. *Methods in Enzymol* 207: 353-368.

Heinemann SH, Rettig J, Graack HR and Pongs O (1996). Functional characterization of K_v channel β-subunits from rat brain. *J Physiology* 493.3: 625-633.

Hille B (1992). Ionic channels of excitable membranes. Sinauer, Sunderland, MA.

Hodgkin AL, and Huxley AF (1952a). The components of membrane conductance in the giant axon of *Loligo*. *J Physiology (London)* 116: 473-496.

Hodgkin AL, and Huxley AF (1952b). The dual effect of membrane potential on Na^+ conductance in the giant axon of *Loligo*. *J Physiology* 116: 497-506.

Hodgkin AL, and Huxley AF (1952c). A quantitative description of membrane current and its application to conduction and excitation in nerve. *J Physiology (London)* 117:500-544.

Horn R, and Lange K (1983). Estimating kinetic constants from single channels data. *Biophys J* 43:207-223.

Hoshi T and Zagotta WN (1993). Recent advances in the understanding of K^+ channel function. *Current Opinion in Neurology* 3: 283-290.

Hoshi T, Zagotta WN and Aldrich RW (1990). Biophysical and molecular mechanisms of *Shaker* K^+ channel inactivation. *Science* 250:533-538.

Hoshi T, Zagotta WN and Aldrich RW (1991). Two types of inactivation in Shaker K^+ channels: effects of alterations in the carboxy-terminal region. *Neuron* 7: 547-556.

Hoshi T, Zagotta WN and Aldrich RW (1994). *Shaker* K^+ channel gating I: Transitions near the open state. *J Gen Physiol* 103: 249-278.

Kalbfleisch JG (1985). Statistical inference. Vol. 2 Springer-Verlag. New York 360.

Kamb A, Iverson LE, and Tanouye MA (1987). Molecular characterization of *Shaker*, a *Drosophila* gene that encodes a K^+ channel. *Cell* 50: 405-413.

Kamb A., Tseng CJ, and Tanouye MA (1988). Multiple products of the *Drosophila Shaker* gene may contribute to K^+ channel diversity. *Neuron*. 1:421-430.

Kandel ER, Schwartz JH and Jessell TM (2000). Principles of neural science. 4th ed. McGraw-Hill.

Kaplan WD and Trout WE (1969). The behavior of four neurological mutants of *Drosophila*. *Genetics* 61: 399-409.

Kavanugh MP, Hurst RS, Yakel J, Varnum MD, Adelman JP and North RA (1992). Multiple subunits of a voltage-dependent K^+ channel contribute to the binding site for tetraethylammonium. *Neuron* 8: 1-20.

Keynes RD and Rojas E (1974). Kinetics and steady-state properties of the charged system controlling Na^+ conductance in the squid giant axon. *J Physiol. (London)* 239: 393-434.

Koch MC, Steinmeyer K, Lorenz C, Ricker K, Wolf F, Otto M, Zoll B, Lehmann-Horn F, Grzeschik KH and Jentsch TJ (1992). The skeletal muscle Cl^- channel in dominant and recessive human myotonia. *Science* 257: 797-800.

Li M, Unwin N, Stauffer KA, Jan YN and Jan LY (1994). Images of purified *Shaker* K^+ channels. *Curr Biol* 4: 110-115.

Liman ER, Tytgat J and Hess P (1992). Subunit stoichiometry of a mammalian K^+ channel determined by construction of multimeric cDNAs. *Neuron* 9: 861-871.

Litt M, Kramer P, Browne D, Gancher S, Brunt ERP, Root D, Phromchotikul T, Dubay CJ and Nutt J (1994). A gene for episodic ataxia / myokymia maps to chromosome 12p13. *Am J Hum Genet* 55: 702-709.

Liu Y, Jurman ME and Yellen G (1996). Dynamic rearrangement of the outer mouth of a K^+ channel during gating. *Neuron* 16: 859-867

Llano I and Gerschenfeld HM (1993). Beta-adrenergic enhancement of inhibitory synaptic activity in rat cerebellar stellate and Purkinje cells. *J Physiol* 468: 201-224.

Lopez GA, Jan YN, Jan LY (1991). Hydrophobic substitution mutations in the S4 sequence alter voltage-dependent gating in *Shaker* K^+ channels. *Neuron* 7: 327-336.

MacKinnon R (1991). Determination of the subunit stoichiometry of a voltage-activated K^+ channel. *Nature* 350: 232-23

Noda M, Shimizu S, Tanabe T, Takai T, Kayano T, Ikeda T, Takahashi H, Nakayama H, Kanaoka Y, Minamino N, Kahugawa K, Matsuo H, Raftery MA, Hirose T, Inayama S, Hayashida H, Miyata T, and Numa S (1984). Primary

structure of electrophorus electricus Na^+ channels deduced from cDNA sequence. *Nature* 312: 121-127.

Pak MD, Baker K, Covarrubias M, Butler A, Ratcliffe A and Salkoff L (1991). MShal, a subfamily of A-type K^+ channel cloned from mammalian brain. *Proc Natl Acad Sci* 88: 4386-4390.

Papazian DM, Schwarz TL, Tempel BL, Jan YN, and Jan LY (1987). Cloning of genomic and complementary DNA from *Shaker*, a putative K^+ channel gene from *Drosophila*. *Science* 237: 749-753.

Papazian DM, Timpe LC, Jan YN and Jan LY (1991). Alteration of voltage-dependence of *Shaker* K^+ channel by mutations in the S4 sequence. *Nature* 349: 305-310.

Parcej DN, Scott VES and Dolly JO (1992). Oligomeric properties of α dendrotoxin-sensitive K^+ ion channels purified from bovine brain. *Biochemistry* 31: 11084-11088.

Pongs O, Kecskemethy N, Muller R, Krah JI, Baumann A, Kiltz HH, Canal I., Llamazares S, and Ferrus A (1988). *Shaker* encodes a family of putative K^+ channel proteins in the nervous system of *Drosophila*. *EMBO J* 7: 1087-1096.

Ptacek L (1994). Ion channel Shake-down. Nature Genetics 8: 111-112.

Ptacek LJ, Tawil R, Griggs RC, Engel AG, Layzer RB, Kwiecinski H, McManis PG, Santiago L, Moore M, Fouad G (1994). Dihydropyridine receptor mutations cause hypokalemic periodic paralysis. *Cell* 77: 863-868.

Rettig J, Heinemann SH, Wunder F, Lorra C, Parcej DN, Dolly JO and Pongs O (1994). Inactivation properties of voltage-gated K^+ channels altered by presence of β-subunit. *Nature* 369: 289-294.

Ruppersberg JP, Schroter KH, Sakmann B, Stocker M, Sewing S, and Pongs O (1990). Heteromultimeric channels formed by rat brain K^+ channel proteins. *Nature* 345: 535-537

Sakmann B and Neher E (1995). Single-Channel Recording. 2nd Ed. Plenum Press, New York and London.

Salkoff L, Baker K, Butler A, Covarrubias M, Pak MD and Wei A (1992). An essential "set" of K^+ channels conserved in flies, mice and humans. *Trends in Neurosciences* 15: 161-166.

Schoppa NE, and Sigworth FJ (1998a). Activation of *Shaker* K^+ channels I. characterization of voltage-dependent transitions. *J Gen Physiol* 111: 271-294

Schoppa NE, and Sigworth FJ (1998b). Activation of *Shaker* K^+ channels II. Kinetics of the V2 mutant channel. *J Gen Physiol* 111: 295-311

Schoppa NE, and Sigworth FJ (1998c). Activation of *Shaker* K^+ channels III. An activation gating model for wild-type and V2 mutant channels. *J Gen Physiol* 111: 313-342

Schroter KH, Ruppersberg JP, Wunder F, Rettig J, Stocker M and Pongs O (1991). Cloning and functional expression of a TEA-sensitive A-type K^+ channel from rat brain. *FEBS letters* 278: 211-216.

Shi G, Nakahira K, Hammond S, Rhodes KJ, Schechter LE and Trimmer JS (1996). β subunits promote K^+ channel surface expression through effects early in biosynthesis. *Neuron* 16: 843-852

Sigworth FJ and Sine SM (1987). Data transformations for improved display and fitting of single-channel dwell time histograms. *Biophys J* 52: 1047-1054.

Stuhmer W, Stocker M, Sakmann B, Seeburg P, Baumann A, Grupe A, and Pongs O (1988). K^+ channels expressed from rat brain cDNA have delayed rectifier properties. *FEBS* 242: 199-206.

Stuhmer W, Conti F, Suzuki H, Wang XD, Noda M, Yahagi N, Kubo H and Numa S (1989). Structural parts involved in activation and inactivation of the Na^+ channel. *Nature* 339: 597-603.

Stuhmer W, Ruppersberg JP, Schroter KH, Sakmann B, Stocker M, Giese KP, Perschke A, Baumann A and Pongs O (1989). Molecular basis of functional diversity of voltage-gated K^+ channels in mammalian brain. *EMBO J* 8: 3235-3244.

Tempel BL, Jan YN, and Jan LY (1988). Cloning of a probable K^+ channel gene from mouse brain. *Nature* 332: 837-839.

Tempel BL, Papazian DM, Schwarz TL, Jan YN, Jan LY (1987). Sequence of a probable K^+ channel component encoded at *Shaker* locus of *Drosophila*. *Science* 14;237:770-775.

Tsien RW, Ellinor PT and Horne WA (1991). Molecular diversity of voltage-dependent Ca^{2+} channels. *Trends in Pharmacological Sciences* 12: 349-354.

Vahedi K, Joutel A, Bogaert PV, Ducros A, Maciazeck J, Bach JF, Bousser, MG and Tournier-Lasserve E (1995). A gene for hereditary paroxysmal cerebellar ataxia maps to chromosome 19p. *Ann Neurol* 37: 289-293.

Wang H, Kunkel DD, Martin TM, Schwartzkroin PA, Tempel BL (1993). Heteromultimeric K+ channels in terminal and juxtaparanodal regions of neurons. *Nature* 365: 75-79.

Wang H, Kunkel DD, Schwartzkroin PA, Tempel BL (1994). Localization of Kv1.1 and Kv1.2, two K channel proteins, to synaptic terminals, somata, and dendrites in the mouse brain. *J Neurosci* 8:4588-4599.

Wei A, Jegla T and Salkoff T (1996). Eight K^+ Channel Families Revealed by the *C. elegans* Genome Project. *Neuropharmacol* 35: 805-829.

Yang N, George AL and Horn R (1996). Molecular basis of charge movement in voltage-gated Na^+ channels. *Neuron* 16: 113-122.

Zagotta WN, Hoshi T and Aldrich RW (1989). Gating of single *Shaker* K^+ channels in *Drosophila* muscle and in Xenopus oocytes injected with *Shaker* mRNA. *Proc Natl Acad Sci* 86: 7243-7247.

Zagotta WN, Hoshi T and Aldrich RW (1990). Restoration of inactivation in mutants of *Shaker* K^+ channels by a peptide derived from ShB. *Science* 250: 568-571.

Zagotta WN, Hoshi T, Dittman J and Aldrich RW (1994). *Shaker* K^+ channel gating II: transitions in the activation pathway. *J Gen Physiol* 103: 279-319

Zagotta WN, Hoshi T and Aldrich RW (1994). *Shaker* K^+ channel gating III: evaluation of kinetic models for activation. *J Gen Physiol* 103: 321-362.

Zerr P, Adelman JP, and Maylie J (1998). Episodic ataxia mutations in Kv1.1 alter K^+ channel function by dominant negative effects or haploinsufficiency. *J Neuroscience* 18: 2842-2848.

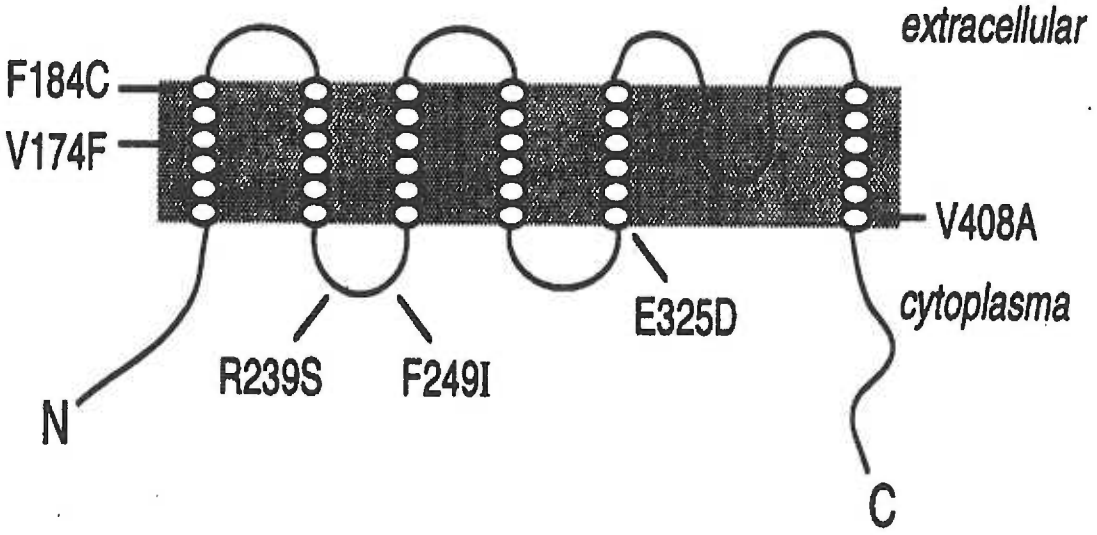

Figure 1. Schematic representation of the membrane topology of Kv1.1 subunits. The positions of the EA-1 missense point mutations are indicated. Number sequences refer to the position of amino acids, letters refer to the amino acids from the originals to the EA-1 mutations. All EA-1 mutations were found in the EA families. The different locations of the various EA-1 point missense mutations suggest that they may affect distinct aspects of voltage-gated K^+ channels. Furthermore, they occur at positions that are highly conserved among the voltage-dependent K^+ channels. Two mutations (V174F and F184C) reside in the first transmembrane domain (S1), two (R239S and F249I) in the intracellular loop between S2 and S3, one (E325D) at the cytoplasmic interface of S5, and one (V408A) in the C-terminal portion of S6 [Adapted from Adelman, Bond, Pessia and Maylie, 1995].

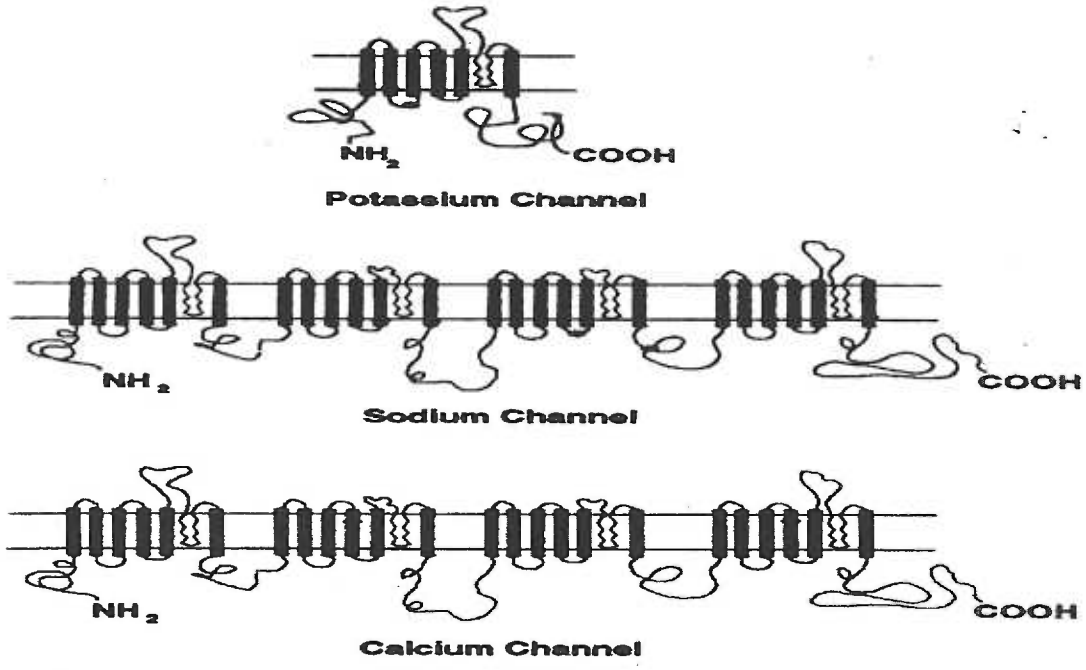

Figure 2. Putative transmembrane topology of voltage-gated K^+, Na^+ and Ca^{2+} channels. Voltage-gated K^+, Na^+ and Ca^{2+} channels share significant similarities. The genes that encode these cation channels are evolutionarily related and form a large gene family. The amino acid sequence of the voltage-gated Na^+ and Ca^{2+} channels contains four homologous domains, each containing six putative transmembrane segments, including one S4 segment and one P loop. The amino acid sequence of most voltage-gated K^+ channels is only approximately one fourth as long as those of voltage-gated Na^+ and Ca^{2+} channels and contains only a single S4 segment (Kamb, Tseng, and Tanouye, 1988; Pongs, Kecskemethy, Muller, Krah, Baumann, Kiltz, Canal, Llamazares, and Ferrus, 1988). Therefore, the K^+ channel peptide is thought to represent only a subunit of a multimeric voltage-dependent K^+ channel (MacKinnon, 1991) [Adapted from Ptacek, 1994].

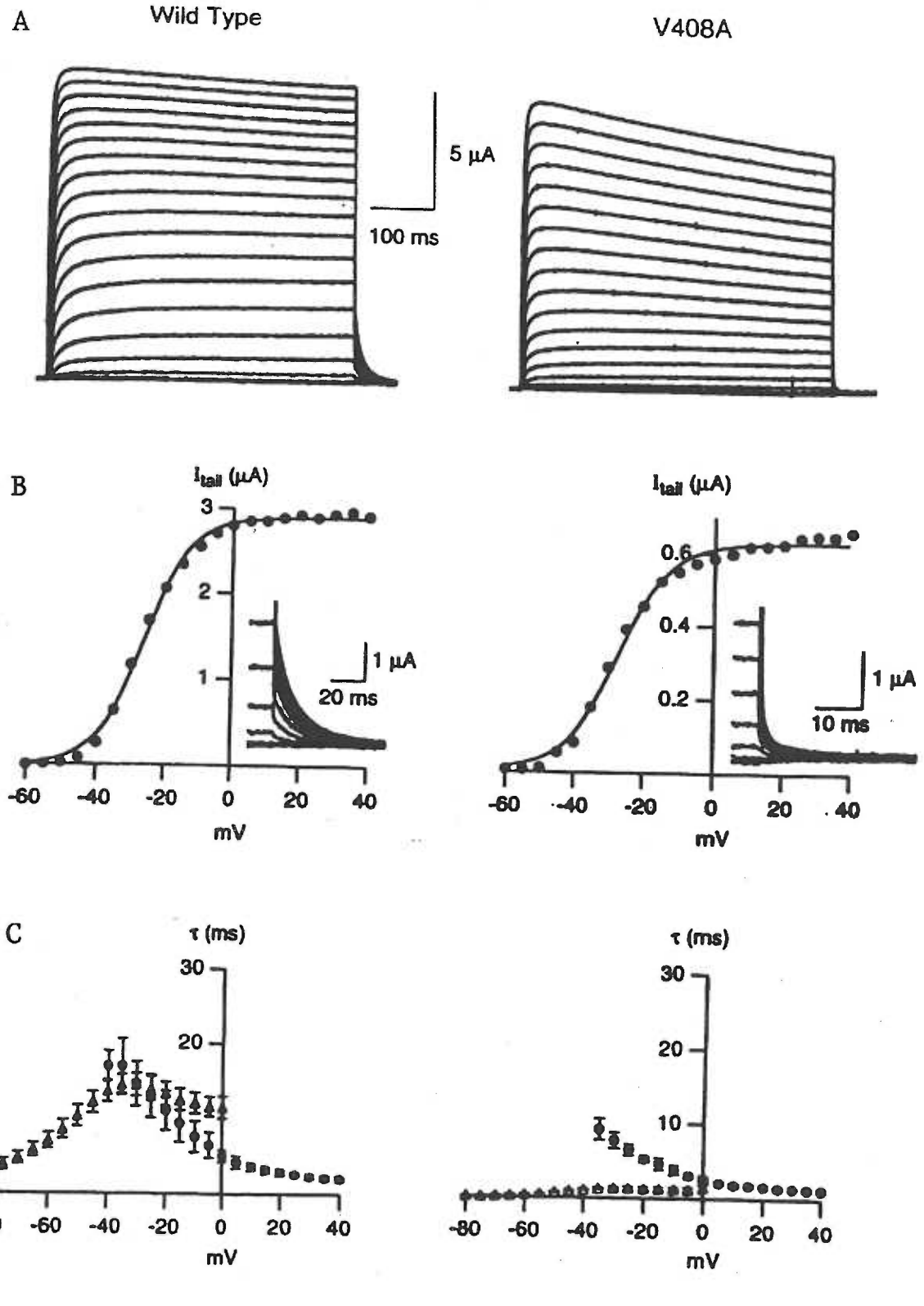
A
Wild Type
V408A
5 µA
100 ms
B
I_{tail} (µA)
3
2
1
1 µA
20 ms
-60
-40
-20
0
20
40
mV
I_{tail} (µA)
0.6
0.4
0.2
1 µA
10 ms
-60
-40
-20
0
20
40
mV
C
τ (ms)
30
20
-80
-60
-40
-20
0
20
40
mV
τ (ms)
30
20
10
-80
-60
-40
-20
0
20
40
mV

Figure 3. Current families and voltage dependence of activation for wild type and V408A channels from two-electrode voltage-clamp recordings. (A) Current families evoked by 500 ms depolarizing commands from ¨ 60 to +40 mV delivered in 5 mV increments from a holding of ¨ 80 mV. Note that V408A has increased C-type inactivation. (B) Tail current amplitudes were measured immediately after the capacitive transient current (~1 ms). Tail currents were recorded at ¨ 60 mV (wild type) or ¨ 45 mV (V408A). The data points were plotted as a function of the command potential and fitted with a Boltzmann function. Inset shows expanded views of the tail currents. Note the faster deactivation rates for V408A channels. (C) Activating and deactivating current traces were fitted with exponential functions. Activation (*filled symbols*) required two exponentials; deactivation (*open symbols*) required only a single exponential. V408A channels activate approximately 2- to 3- fold faster than wild type channels. Deactivation is 10-fold faster for V408A channels than for wild type at all voltages and is more voltage dependent [Adapted from Adelman, Bond, Pessia and Maylie, 1995].

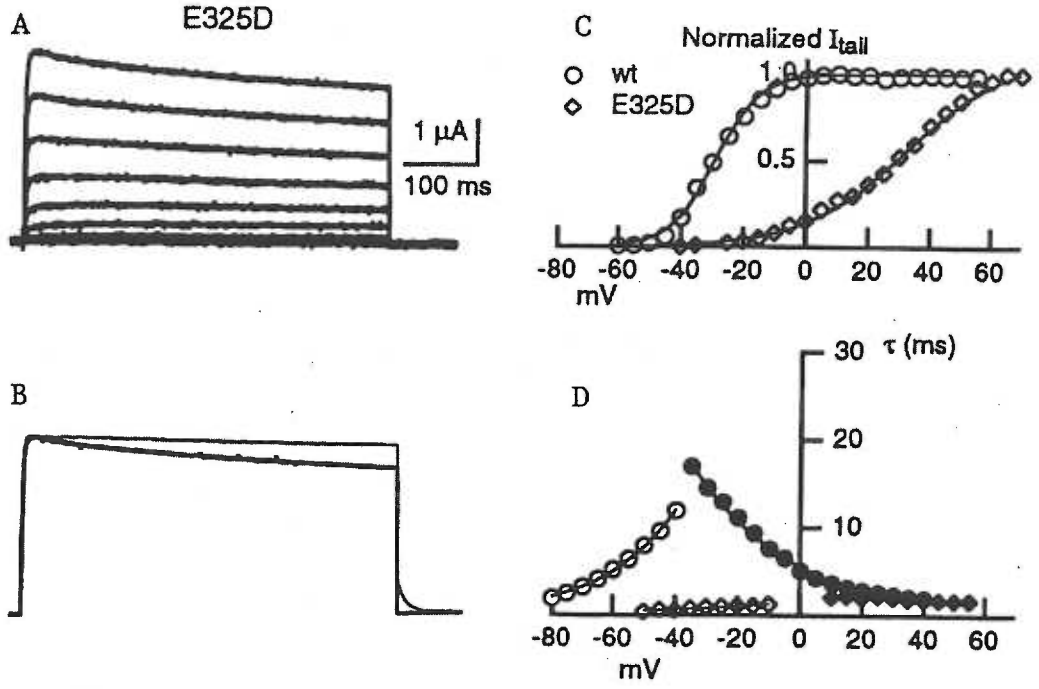

Figure 4. Voltage dependence of activation for wild type and E325D channels. (A) Traces representing currents of one E325D recording evoked from ¨ 60 to 50 mV depolarizing pulses (increments of 10 mV) from a holding potential of ¨ 80 mV. Tail currents were recorded at ¨ 50 mV. (B) Current traces for E325D (*thick lines*) was scaled and superimposed to a representative wild type current trace (*thin lines*). Currents were evoked at 40 mV from a holding potential of ¨ C 80 mV, and tail currents were recorded at ¨ 50 mV. (C) Voltage dependence of activation from a single representative experiment with wild type and E325D channels. The normalized tail currents recorded at ¨ 50 mV were plotted as a function of the preceding depolarizing potential (-60 to 65 mV). The tail currents were fitted with a single exponential, and the amplitude of the exponential was used to describe the tail currents. Data points were fitted according to the Boltzmann equation $I = 1/(1 + \exp^{-(V-V1/2)/k})$, where $V_{1/2}$ is the potential of half-activation, and *k* is a slope factor. (D) Time constant of activation (*filled symbols*) and deactivation (*open symbols*) from a single representative experiment. Activation of currents was best described with a sum of two exponentials, and the time constant of the fast exponential was plotted here, whereas a single

exponential was sufficient for the deactivation. Data points were fitted according to the equation $\tau = \tau_{v1/2} e^{(V-V1/2)/k}$, where $\tau_{v1/2}$ is the time constant at $V_{1/2}$, and k is the slope factor for the voltage dependence of the time constant [Adapted from Zerr, Adelman, and Maylie, 1998].

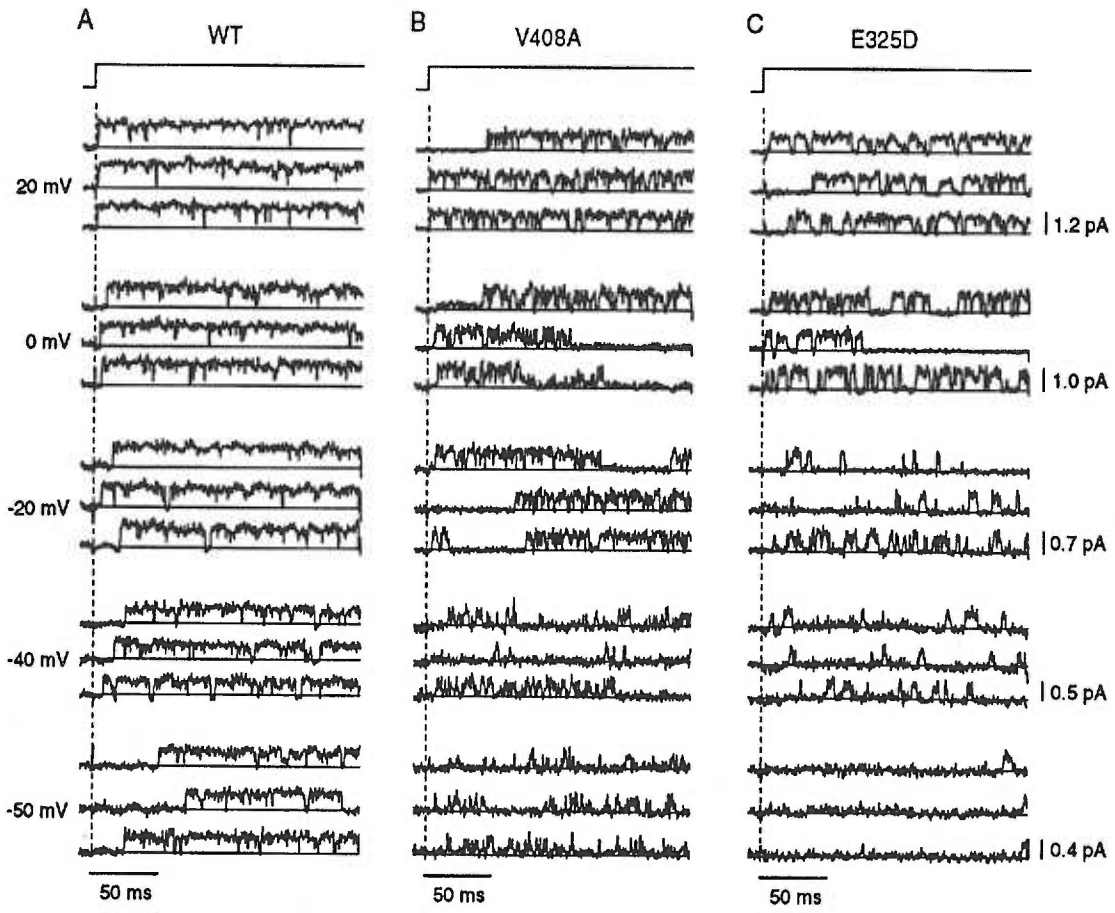

Figure 5. Representative single-channel current traces from wild type (A), V408A (B) and E325D (C) elicited in response to 200 ms depolarizing voltage pulses to different potentials from a holding potential of ¨ 80 mV are shown. All three channels reveal a latency to first opening (delay between vertical dashed line and first opening) that appears to decrease with increasing voltage. Wild type channels do not enter a long duration closed state after opening consistent with the lack of N-type inactivation and minimal C-type inactivation. However, some of the traces from V408A and E325D channels reveal a long closed state after opening that may reflect the faster C-type inactivation for these mutations. Further, comparison of the traces at similar depolarizing voltages reveal that after opening V408A and E325D channels flicker between open and closed state more often than wild type indicative of a destabilized open state.

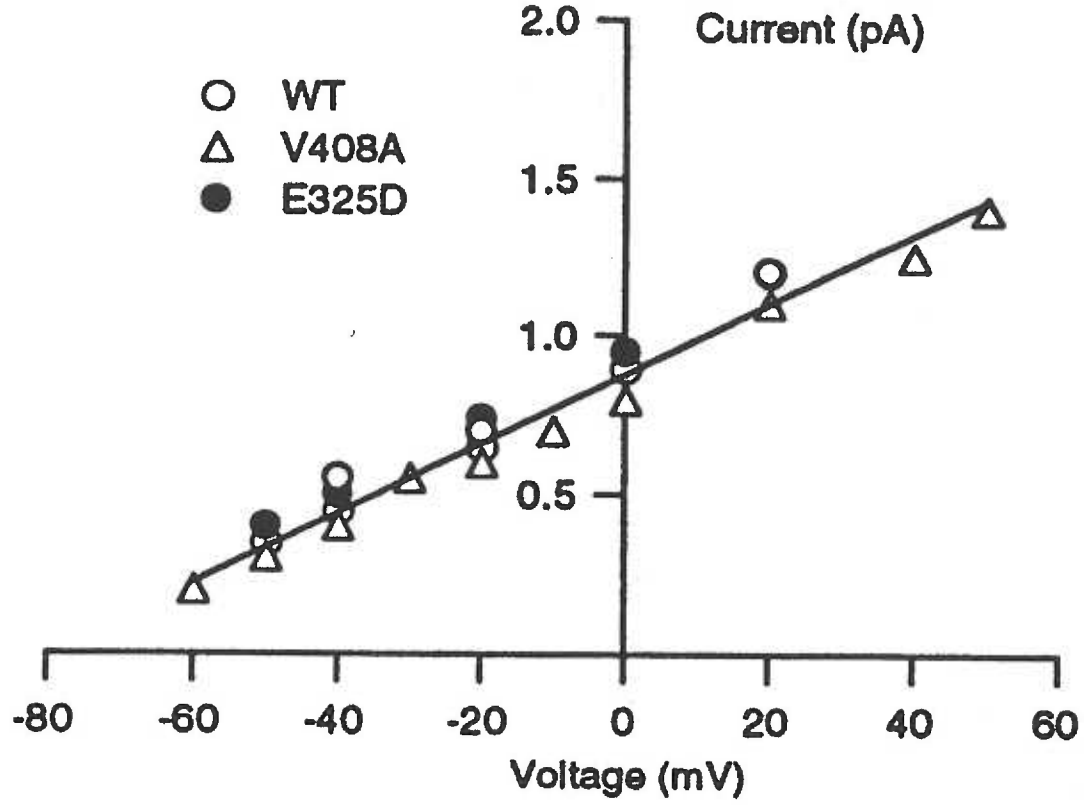

Figure 6. Single-channel conductance for wild type, V408A and E325D channels. This shows that wild type, V408A and E325D channels enter a single conductance state within the time course of the recordings. Single channel currents were determined from an all point histogram at each voltage and plotted versus membrane potential (Fig. 5). For comparison a line with a slope conductance of 10.5 pS was drawn on the graph. The single-channel conductance (pS) for wild type, E325D and V408A were 10.5$\pm$0.459 (n=5), 10.5$\pm$0.786 (n=3) and 10.0$\pm$0.577 (n=3), respectively. This result shows that the EA-1 mutations, V408A and E325D, do not affect the single channel conductance and that the reduction in whole cell current observed with these EA-1 mutations is not the result of a decreased single channel conductance.

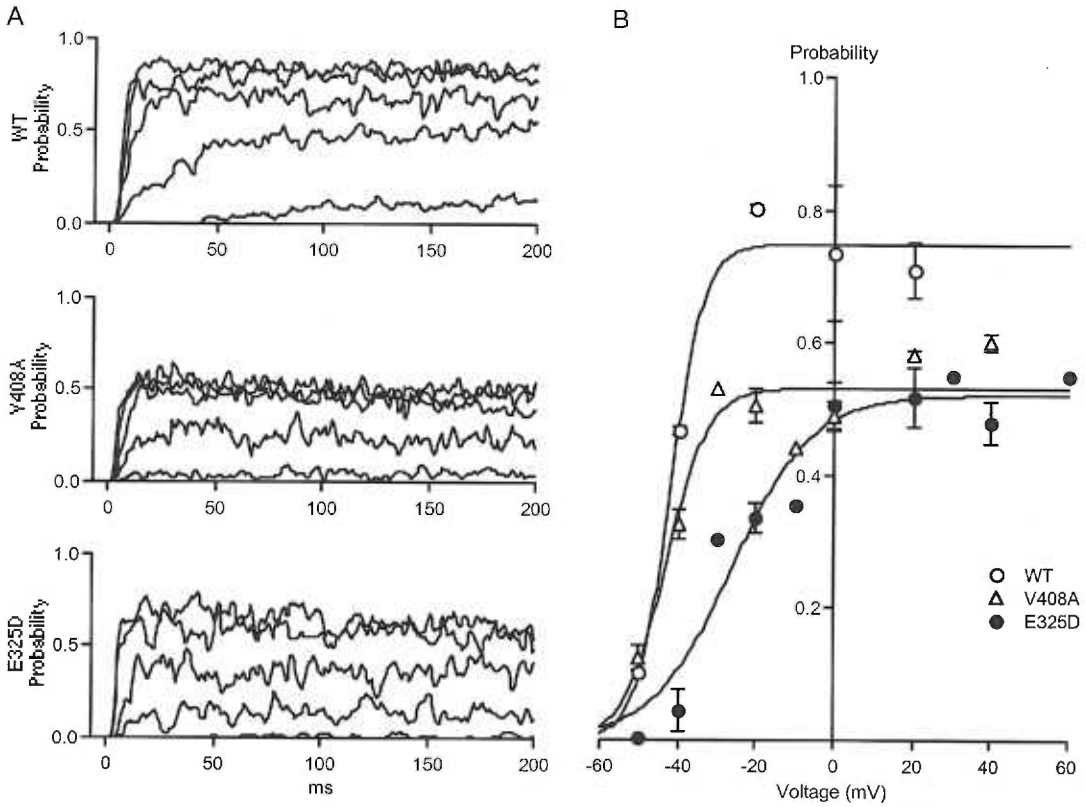

Figure 7. (A) The average behavior of the channels in the ensemble averages from representative single patches of wild type, V408A and E325D channels. Ensemble traces were constructed from the average of all the sweeps at each depolarizing voltage from ¨ 60 mV to 60 mV. The time course of the probability relaxation to steady state became more rapid and the probability the channel was open increased for depolarization from ¨ 60 to -10 mV. Moreover, the open probability did not exhibit a time-dependent decay suggesting that C-type inactivation does not compromise the data on this time scale. (B) Plot of the steady-state open probability that the channel is open as a function of voltage from all the patches of wild type (n=5), V408A (n=3) and E325D (n=3). The data were fitted with a single Boltzmann distribution. The voltage at which half the channels were open, $V_{1/2}$, was -42 mV for wild type and -43 mV for V408A. E325D shifted the $V_{1/2}$ to -26 mV and reduced the steepness factor from 4 to 10 mV consistent, but not as dramatic, as that determined from the whole oocyte

using two-electrode voltage clamp.

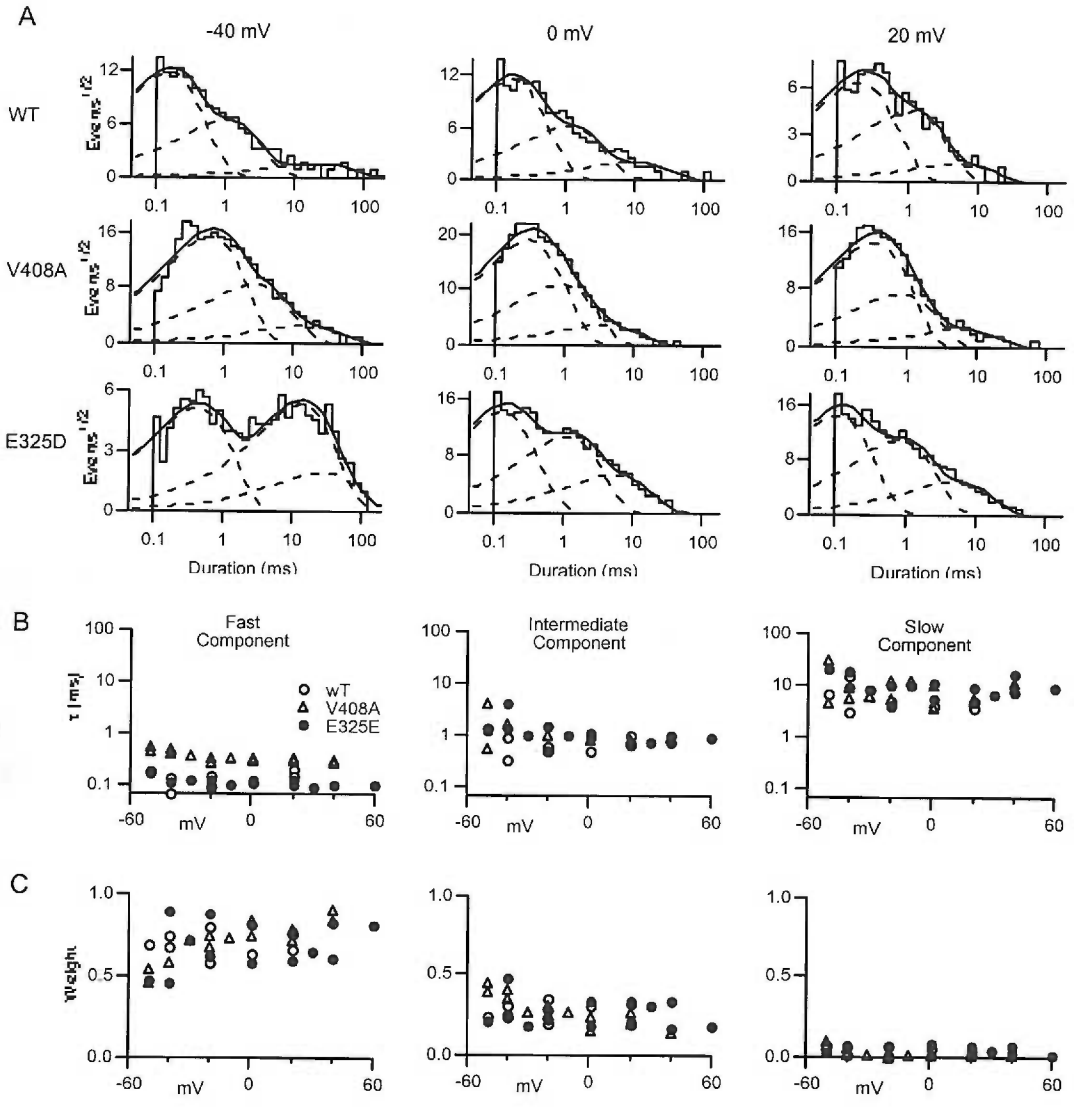

Figure 9. (A) Closed duration histograms measured at different voltages from single representative patches of wild type, V408A and E325D channels. The data were fitted with a sum of three exponentials. The solid line represents the overall fitted curves and the dashed lines indicate the underlying individual components. Voltage dependence of the time constants (B) and relative amplitudes (C) of the

three exponential components from all the patches of wild type (n=5), V408A (n=3) and E325D (n=3). Wild type and EA-1 mutations all have 3 components. There is no difference between wild type and V408A or E325D channels. The fast component, 0.3 ms in duration, can be seen as flicker closings in the single channel records. These closings represent the most frequently observed closed events, over 70% of the closures. The duration and frequency of these events is only weakly dependent on voltage between ¨ 60 and +60 mV. The intermediate component of the distribution of closed durations is 1 to 5 ms in duration and comprises about 30% of the closures. Its time constant and relative amplitude also display very little voltage dependence between ¨ 60 and +60 mV. In contrast to the fast and intermediate components, the slow component is frequently not significant at depolarized voltages and is more prevalent in the activation voltage range, at ¨ 40 mV and ¨ 60 mV, than at the depolarized voltages.

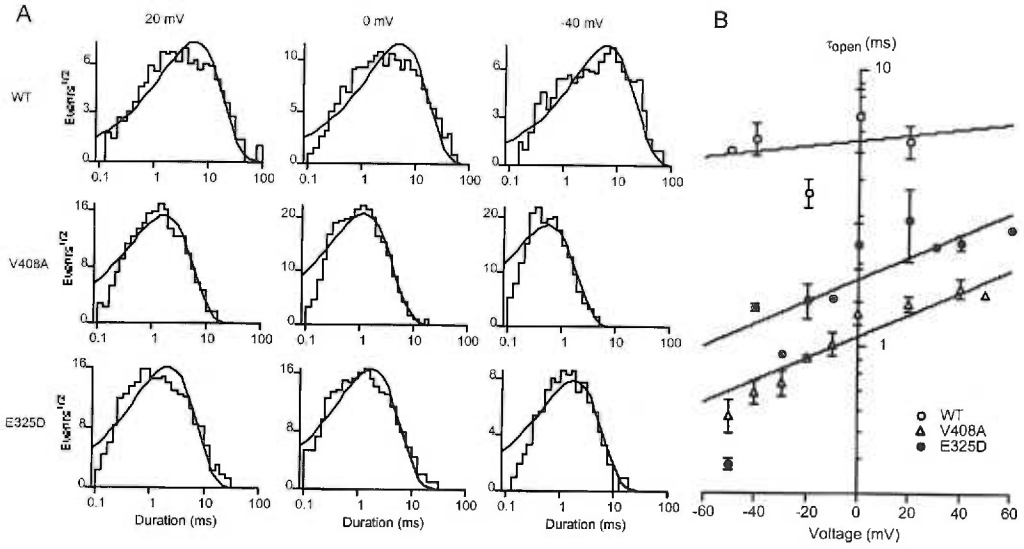

Figure 10. (A) Open duration histograms at different voltages from single representative patches of wild type, V408A and E325D channels. In all patches the open events elicited by steps to voltages between ¨ 60 and +50 mV were sufficiently described by a single exponential distribution and did not warrant a distribution containing two components. This suggests that only a single open conformation is kinetically distinguishable in the wild type, V408A and E325D channels. (B) Voltage dependence of the time constants of the open durations from all the patches of wild type (n=5), V408A (n=3) and E325D (n=3). The mean open duration of wild type has no voltage dependence between ¨ 60 and +50 mV. This result is consistent with the *Shaker* K^+ channel study (Hoshi, Zagotta and Aldrich, 1994). However, the mean open duration of the two EA-1 mutations, E325D and V408A, was voltage dependent between ¨ 60 and +50 mV.